

# Glass viscosity calculation based on a global statistical modelling approach

Alexander Fluegel<sup>1</sup>

Pacific Northwest National Laboratory, Richland, Washington, USA

Date received 17 July 2006

Revision received 14 February 2007

Accepted 17 February 2007

*A viscosity model for predicting the complete viscosity curve of glass was developed using a global statistical approach and more than 2200 composition–viscosity data for silicate glasses collected from over 50 years of scientific literature, including soda–lime–silica container and float glasses, TV panel glasses, borosilicate fibre wool and E type glasses, low expansion borosilicate glasses, glasses for nuclear waste vitrification, lead crystal glasses, binary alkali silicates, and various other compositions. It is shown that, within a measurement series from a specific laboratory, the reported viscosity values are commonly overestimated at higher temperatures due to evaporation losses during the measurement and glass preparation; this includes data presented by Lakatos et al (1972) and the recent ‘High temperature glass melt property database for process modelling’ by published by Seward et al (2005). Similarly, in the glass transition range many experimental data reported for borosilicate glasses are too high due to phase separation effects. The global model developed here corrects those errors. The model standard error was 9–17°C, with  $R^2=0.985–0.989$ . The prediction confidence interval in mass production largely depends on the glass composition of interest, the composition uncertainty, and the viscosity level. The mixed alkali effect for the viscosity is derived from nonlinear alkali–silica interactions in binary systems.*

## 1. Introduction

The objective of this paper is to develop an accurate glass viscosity model relevant to commercial application through statistical analysis and based on all composition–property data available in SciGlass.<sup>(1)</sup> The source data in SciGlass originate from numerous scientific and technical publications from several decades of research that do not always agree. The goal in this study is to evaluate and correct systematic differences between data from specific investigators, thereby making comparable a large number of data series and previous viscosity models, creating a broadly founded accuracy, and increasing the reliability of viscosity predictions. A detailed error calculation, sensitive to the glass composition of interest, is intended to provide a dependable viscosity prediction confidence interval for estimating process tolerances in the industry.

Viscosity,  $\eta$ , is probably the most important property in glass making; it strongly influences the melting and fining conditions in glass furnaces, which are correlated with the furnace energy consumption. During glass forming processes the viscosity must be tightly controlled to maintain a high product quality. The temperatures throughout the glass cooling schedule are dictated by the viscosity.

Systematic studies of the viscosity–temperature relation in glasses were initiated by Vogel,<sup>(2)</sup> Fulcher<sup>(3)</sup> and Tammann *et al.*,<sup>(4)</sup> and resulted in the now widely accepted Vogel–Fulcher–Tammann (VFT) Equation:

$$\log(\eta)=A+B/(T-T_0) \quad (1)$$

The viscosity depends on the chemical glass composition as well as temperature. As early as the 1920s, English<sup>(5)</sup> and Gehlhoff *et al.*<sup>(6)</sup> were engaged in studies of soda–lime–silica glasses to establish the sensitivity of viscosity to compositional changes.

It would be very convenient to be able to calculate viscosity and its variation with temperature from the chemical composition of a glass. Numerous publications are devoted to this topic,<sup>(7–33)</sup> and have been summarised by Scholze,<sup>(34)</sup> Volf<sup>(35)</sup> and Martlew,<sup>(36)</sup> the data from such publications have recently been incorporated in the SciGlass information system.<sup>(1)</sup> The programs SciGlass<sup>(1)</sup> and Interglad<sup>(37)</sup> are equipped with an automated simple linear multiple regression feature for the glass properties they contain. Among the mentioned models, probably most widely used at present are the empirical approaches of Lakatos *et al.*<sup>(7)</sup> (soda–lime–silica, borosilicate fibre, lead crystal), and Fluegel *et al.*<sup>(32)</sup> (soda–lime–silica, TV panel, borosilicate fibre wool and E type, low expansion borosilicate).

Viscosity models that are not based on the directly empirical method,<sup>2</sup> such as the thermodynamic ap-

<sup>1</sup> Email address: fluegel@gmx.com

Proceedings of the Eighth International Conference on Advances in Fusion and Processing of Glass, 12–14 June 2006, Dresden, Germany

proach of Conratt,<sup>(22)</sup> are not intended to provide accurate predictions in the first place, but to demonstrate property relations. Therefore, the accuracy of the directly empirical viscosity models described in this paper cannot be compared to non-empirical models. The directly empirical method allows the highest accuracy, considering the limits of validity for the model.

For direct empirical modelling most investigators use their own viscosity measurements as the sole data source; sometimes findings from another investigator who is in good agreement are also considered, such as in the models by Öksoy *et al.*<sup>(23)</sup> and Fluegel *et al.*<sup>(32)</sup> This approach has the advantage that the models obtained describe the source data very well. However, important issues remain unresolved.

Experimental viscosity data from various laboratories can differ by 50°C or more, even within simple glass systems as shown in Figure 1. (Figure 1 also shows model predictions based on the present work for later discussion.) Naturally, disagreements in the data for commercial multicomponent glasses may be substantially larger than for simple binary glasses; however, most experimental data for multicomponent glasses are not directly comparable because of differences in the compositions studied.

As a result of the disagreements between experimental data from different laboratories, the models derived from those data are also in conflict.<sup>(34)</sup> For example, predictions from several models of the

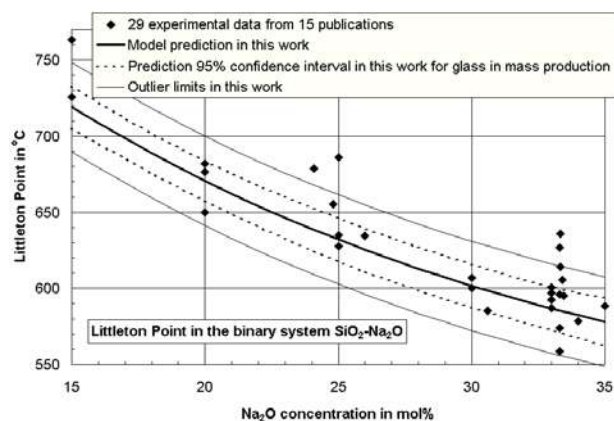


Figure 1. Temperatures at a constant viscosity level of  $\log(\eta/(\text{Pa}\cdot\text{s}))=6.6$  (~Littleton Softening Point) in the binary system  $\text{SiO}_2\text{-Na}_2\text{O}$ , based on all 29 available data in SciGlass<sup>(1)</sup> for  $c(\text{Na}_2\text{O})=15\text{-}35$  mol%. The diagram also shows the model predictions in this work. The model does not follow the best fit for the given 29 data points in the binary system  $\text{SiO}_2\text{-Na}_2\text{O}$  because, in addition, hundreds of other data are considered in the model

<sup>2</sup> Strictly speaking, all glass property models are empirical by nature because all are based on observations of one kind or another. Besides the thinking process itself, nothing is perceived 'ab initio'. In this paper, the 'directly empirical modelling method' is defined as mathematical analysis and interpretation of only one property, without invoking another property as basis (not considering the molecular mass and the chemical valency).

glass melting point in °C at a viscosity of 10 Pa s (100 Poise) for the compositions given in Table 1 are listed in Table 2. All glasses in Table 1 are standards, where the viscosity (but not the composition except for DGG I) has been verified by several laboratories, excluding the soda–lime–silica container glass 'CO'. CO is listed because of its simple composition, which is covered by most viscosity models. The experimental results are also shown in Table 2 for comparison.

The few direct empirical viscosity models, that consider papers by several investigators as data sources, were published by Bottinga *et al.*,<sup>(15)</sup> Lyon<sup>(14)</sup> and Fluegel *et al.*<sup>(31)</sup> However, in these three papers only a small fraction of the available viscosity data currently available are considered, and the statistical modelling procedure used is not developed in detail. The viscosity model of Priven<sup>(1,28)</sup> is derived from all data available in the literature for unary, binary, and ternary glass systems, and uses multicomponent glasses for verification purposes only. The advantage of Priven's model lies in its practically unlimited application;<sup>3</sup> however, it sacrifices accuracy in detail. The automated simple linear multiple regression features in the databases SciGlass<sup>(1)</sup> and Interglad<sup>(37)</sup> are not comparable to a careful statistical analysis carried out by an expert.

No viscosity model known to the author quantifies precisely the error in the predictions for the glass composition of interest, considering the results of many investigators. The prediction errors of models based on data from one single laboratory are not necessarily valid for other laboratories.<sup>(32)</sup> In the models of Bottinga *et al.*,<sup>(15)</sup> Lyon,<sup>(14)</sup> Priven<sup>(28)</sup> and Fluegel *et al.*<sup>(31)</sup> some overall errors are reported, but prediction errors valid for a specific composition are not given.

Systematic differences between viscosity data from different publications have not been investigated, except in earlier papers by the author.<sup>(31,32)</sup>

Most viscosity models use the additivity method wherein the predictions change linearly with the concentrations of the glass components. While this is a good approach within limited composition ranges, it cannot be applied to different glass families simultaneously (such as soda–lime–silica and borosilicate), and therefore, data based on this approach are not comparable over wide composition areas.

## 2. Statistical data analysis

The source data and all references used in this work are given in the SciGlass database.<sup>(1)</sup> References for the larger or otherwise important data series are displayed in Tables 1 and 8–11. All glass compositions were converted to mol%. The concentrations of some

<sup>3</sup> Even though the viscosity model by Priven can be applied to virtually all glasses, the approach itself is not 'global' or 'universal' because of its incremental character.<sup>(28)</sup>

Table 1. Compositions in mol% of glasses for melting point predictions in Table 2

	Soda–lime–silica (CO) container glass <sup>(38)</sup>	NIST 710A <sup>(39)</sup>	NIST 717A <sup>(40)</sup>	711 <sup>(41)</sup>	710 <sup>(42)</sup>	DGG I	Waste glass standard (WGS) <sup>(44)</sup>
SiO <sub>2</sub>	74.41	71.43	72.25	71.28	72.74	70.94	53.76
Al <sub>2</sub> O <sub>3</sub>	0.75	1.31	2.19	0.51	0.11	0.72	3.04
Na <sub>2</sub> O	12.90	8.25	1.03	3.76	8.70	14.34	12.54
K <sub>2</sub> O	0.19	6.27	5.42	5.55	5.07	0.21	1.93
MgO	0.30	-	-	-	-	6.16	1.41
CaO	11.27	9.62	-	-	12.82	7.13	1.77
SO <sub>3</sub>	0.16	-	-	-	0.15	0.32	-
Fe <sub>2</sub> O <sub>3</sub>	0.01	-	-	-	0.01	0.07	6.00
TiO <sub>2</sub>	0.01	0.32	-	-	-	0.10	1.00
ZnO	-	2.81	-	-	-	-	-
B <sub>2</sub> O <sub>3</sub>	-	-	16.97	-	-	-	8.24
Li <sub>2</sub> O	-	-	2.14	-	-	-	7.33
PbO	-	-	-	18.90	-	-	-
Sb <sub>2</sub> O <sub>3</sub>	-	-	-	-	0.40	-	-
MnO <sub>2</sub>	-	-	-	-	-	-	1.84
Cr <sub>2</sub> O <sub>3</sub>	-	-	-	-	-	-	0.04
ZrO <sub>2</sub>	-	-	-	-	-	-	0.06
BaO	-	-	-	-	-	-	0.04
NiO	-	-	-	-	-	-	1.00

transition metals in varying oxidation states were added up to the most common oxidation state. Table 3 lists some constraints imposed during modelling, although the large number of component combination constraints cannot be listed here due to space limitations. All limits are given in detail in Ref. 45. The glass water content varied between 80–642 ppm by weight.<sup>(46)</sup> The original viscosity data were used to interpolate temperatures of constant viscosity (isokom) at log<sub>10</sub>(η/(Pa s))=1.5, 6.6 (~Littleton Softening Point for soda–lime–silica glasses), and 12.0 (close to T<sub>g</sub>). The glass compositions in mol% were employed as independent variables for modelling, while the isokom temperatures were chosen as model responses. This approach has the advantage that no

assumption is made about the temperature–viscosity curve, as opposed to models describing the VFT<sup>(7,23)</sup> or Arrhenius parameters.<sup>(25,33)</sup>

Ideally, it would be desirable not to limit the analysis to only three viscosity levels, as has been done here following the tradition by Lakatos *et al* (*Glass Technol.*, 1972),<sup>(7)</sup> but to include several more with one for each decimal power, e.g. log<sub>10</sub>(η/(Pa s))=0, 1, 2, 3, ... 12. This would provide a very valuable insight about the validity of common temperature–viscosity equations, such as Equation (1), over wide temperature ranges. It is planned to perform this analysis in a forthcoming publication however, because the study of three viscosity levels already gives much material for discussion, it is worthwhile to publish it now. For

Table 2. Predictions from several models of glass melting point and experimental results; the values in parentheses were calculated by slightly exceeding the model validity limits, as is often practiced

Model	Melting point prediction (°C)				DGG I	WGS	
	CO	710A	717A	711			
Experiment	1467	1464	1555	1327	1434	1439	1048
Mazurin <sup>(1,9)</sup>	1440	-	-	-	-	1428	-
Bottinga <sup>(15)</sup>	1494	1525	-	-	1475	1443	-
Lakatos 1972 <sup>(7)</sup>	1478	(1509)	-	-	(1441)	(1458)	-
Lakatos 1976 <sup>(7)</sup>	1473	(1471)	-	-	(1444)	(1456)	-
Lyon <sup>(14)</sup>	1479	(1461)	-	-	(1423)	1454	-
Sasek <sup>(10,34)</sup>	1507	(1590)	-	-	(1493)	1498	-
Ledererova <sup>(13,34,36)</sup>	1529	(1571)	-	-	(1498)	1508	-
Cuartas <sup>(12,34,36)</sup>	(1460)	(1545)	-	-	(1491)	1455	-
Braginskii <sup>(11,34,36)</sup>	(1321)	-	-	-	-	(1436)	-
Herbert <sup>(16)</sup>	-	-	-	1321	-	-	-
Öksoy <sup>(23)</sup>	1438	(290) <sup>a</sup>	-	-	(1406)	(1198) <sup>a</sup>	-
Öksoy <sup>b(23)</sup>	1476	(1494)	-	-	(1437)	(1456)	-
Priven <sup>(1,28)</sup>	1437	1431	1460	1321	1474	1443	(1282)
Fluegel 2004 <sup>(31)</sup>	1478	1465	1558	1323	1434	1452	-
Fluegel 2005 <sup>(32)</sup>	1480	(1534)	-	-	(1472)	(1440)	-
Hrma, 1994 <sup>(25)</sup>	-	-	-	-	-	-	(1075) <sup>c</sup>
Hrma <sup>d</sup> , 2006 <sup>(33)</sup>	1475	-	-	-	-	1437	-
Hrma <sup>e</sup> , 2006 <sup>(33)</sup>	1467	(1433)	(1524)	-	1401	1444	-
This work	1468	1457	1526	1310	1434	1446	1050

<sup>a</sup> unusual predictions caused by the unrealistic coefficients for Fe<sub>2</sub>O<sub>3</sub>, TiO<sub>2</sub>, and SO<sub>3</sub>

<sup>b</sup> neglecting Fe<sub>2</sub>O<sub>3</sub>, TiO<sub>2</sub>, and SO<sub>3</sub>

<sup>c</sup> counting K<sub>2</sub>O as Na<sub>2</sub>O because the model is not valid for glasses containing K<sub>2</sub>O

<sup>d</sup> local model for soda–lime container glasses

<sup>e</sup> global model for various commercial glasses

Table 3. Concentration maxima (mol%) for the source data used in modelling

Component	log( $\eta$ /(Pa.s))			Component	log( $\eta$ /(Pa.s))		
	1.5	6.6	12.0		1.5	6.6	12.0
Ag <sub>2</sub> O	0.0003	0	0	Nd <sub>2</sub> O <sub>3</sub>	1.78	0	0
Al <sub>2</sub> O <sub>3</sub>	11.30	12.70	10.00	NiO	1.87	0	0
As <sub>2</sub> O <sub>3</sub>	0.11	0.11	0.11	P <sub>2</sub> O <sub>5</sub>	4.64	0.85	0
B <sub>2</sub> O <sub>3</sub>	18.15	16.97	16.97	PbO	49.96	50.00	56.00
BaO	10.00	8.00	19.20	PdO	0.001	0	0
Bi <sub>2</sub> O <sub>3</sub>	2.83	0	0	Pr <sub>2</sub> O <sub>3</sub>	0.0005	0	0
CaO	33.47	33.10	50.14	Rb <sub>2</sub> O	0.001	0	0
CdO	0.13	0	0	ReO <sub>2</sub>	0.03	0	0
CeO <sub>2</sub>	3.21	0.30	0.30	Rh <sub>2</sub> O <sub>3</sub>	0.001	0	0
Cl	1.48	0	0	RuO <sub>2</sub>	0.002	0	0
Co <sub>3</sub> O <sub>4</sub>	0.05	0.05	0.05	Sb <sub>2</sub> O <sub>3</sub>	0.17	0.17	0.17
Cr <sub>2</sub> O <sub>3</sub>	0.35	0.16	0.16	Se	0.02	0.02	0.02
Cs <sub>2</sub> O	0.26	0	0	SiO <sub>2</sub> , min.	42.62	42.62	41.40
CuO	2.54	0	0	SiO <sub>2</sub> , max.	89.20	87.10	91.97
Eu <sub>2</sub> O <sub>3</sub>	0.86	0	0	Sm <sub>2</sub> O <sub>3</sub>	0.87	0	0
F	10.31	10.31	4.55	SnO <sub>2</sub>	1.83	0.27	0
Fe <sub>2</sub> O <sub>3</sub>	6.99	2.15	0.57	SO <sub>3</sub>	1.24	0.32	0.33
Ga <sub>2</sub> O <sub>3</sub>	1.10	0	0	SrO	7.37	7.37	18.02
Gd <sub>2</sub> O <sub>3</sub>	1.54	0	0	TeO <sub>2</sub>	0.001	0	0
I	0.08	0	0	ThO <sub>2</sub>	1.46	0	0
K <sub>2</sub> O	41.67	30.00	34.05	TiO <sub>2</sub>	9.26	3.29	25.00
La <sub>2</sub> O <sub>3</sub>	0.42	0	0	UO <sub>2</sub>	4.19	0	0
Li <sub>2</sub> O	35.90	33.30	45.00	V <sub>2</sub> O <sub>5</sub>	2.13	0	0
MgO	16.90	20.00	16.61	WO <sub>3</sub>	0.04	0	0
MnO <sub>2</sub>	3.43	0.18	0.18	Y <sub>2</sub> O <sub>3</sub>	0.91	0	0
MoO <sub>3</sub>	0.33	0	0	ZnO	5.19	8.00	2.81
Na <sub>2</sub> O	44.00	42.00	42.00	ZrO <sub>2</sub>	9.78	2.77	1.76
Nb <sub>2</sub> O <sub>5</sub>	0.01	0	0				

now, the reader is advised to estimate the viscosity levels not discussed here by application of Equation (1). Such estimation is very applicable to commercial glasses (based on earlier studies by the author,<sup>(32)</sup> and on the work of Lakatos *et al* (*Glass Technol.*, 1972),<sup>(7)</sup> who centred his model on log<sub>10</sub>( $\eta$ /(Pa s))=1.5, 6.5, and 11.5). However, very precise measurements below common error limits reveal that the VFT Equation (1) may not be followed exactly; deviations of up to 4°C have been observed for the glass DGG I.<sup>(43)</sup>

Details of the statistical data analysis procedure are described elsewhere.<sup>(32,47-48)</sup> The equation for viscosity predictions is

Isokom temperature =

$$b_0 + \sum_{i=1}^n \left[ b_i C_i + \sum_{k=i}^n \left( b_{ik} C_i C_k + \sum_{m=k}^n b_{ikm} C_i C_k C_m \right) \right] \quad (2)$$

Table 4. Coefficients and t-values at log( $\eta$ /(Pa.s))=1.5

Variable	Coefficient	t-value	Variable	Coefficient	t-value	Variable	Coefficient	t-value
Constant	1824.497	-	Li <sub>2</sub> O	-30.336	-30.42	ZrO <sub>2</sub>	10.173	15.86
Al <sub>2</sub> O <sub>3</sub>	19.341	12.40	(Li <sub>2</sub> O) <sup>2</sup>	0.22499	7.95	B <sub>2</sub> O <sub>3</sub> ×Na <sub>2</sub> O	-0.28237	-7.95
B <sub>2</sub> O <sub>3</sub>	-22.347	-25.97	MgO	-5.038	-12.38	B <sub>2</sub> O <sub>3</sub> ×K <sub>2</sub> O	-0.27890	-3.27
(B <sub>2</sub> O <sub>3</sub> ) <sup>2</sup>	0.60376	11.69	MnO <sub>2</sub>	-17.050	-5.11	B <sub>2</sub> O <sub>3</sub> ×Li <sub>2</sub> O	-0.16843	-3.47
BaO	-18.931	-25.61	K <sub>2</sub> O.MgO	0.59449	2.51	Al <sub>2</sub> O <sub>3</sub> ×Na <sub>2</sub> O	-0.23085	-3.16
Bi <sub>2</sub> O <sub>3</sub>	-42.416	-8.05	Na <sub>2</sub> O	-30.610	-53.42	Al <sub>2</sub> O <sub>3</sub> ×Li <sub>2</sub> O	-0.38421	-3.94
CaO	-17.453	-20.28	(Na <sub>2</sub> O) <sup>2</sup>	0.27887	25.22	Al <sub>2</sub> O <sub>3</sub> ×MgO	-0.44589	-3.53
(CaO) <sup>2</sup>	0.12038	5.09	Nd <sub>2</sub> O <sub>3</sub>	-39.662	-9.41	Al <sub>2</sub> O <sub>3</sub> ×CaO	-0.93909	-12.38
CeO <sub>2</sub>	-22.418	-8.07	PbO	-21.349	-144.74	Na <sub>2</sub> O×K <sub>2</sub> O	0.58773	6.70
Cl	-8.563	-2.33	SO <sub>3</sub>	-13.908	-2.54	Na <sub>2</sub> O×Li <sub>2</sub> O	0.20691	5.64
CuO	-30.913	-5.31	SrO	-17.292	-22.94	Na <sub>2</sub> O×CaO	0.19254	5.61
F	-11.739	-15.51	ThO <sub>2</sub>	-17.185	-2.97	K <sub>2</sub> O×Li <sub>2</sub> O	0.24924	5.98
Fe <sub>2</sub> O <sub>3</sub>	-13.611	-15.81	TiO <sub>2</sub>	-10.323	-13.63	K <sub>2</sub> O×CaO	0.29628	2.78
K <sub>2</sub> O	-31.907	-27.61	UO <sub>2</sub>	-17.672	-6.67	MgO.CaO	-0.17394	-4.19
(K <sub>2</sub> O) <sup>2</sup>	0.61234	9.51	V <sub>2</sub> O <sub>5</sub>	-21.727	-5.80	Al <sub>2</sub> O <sub>3</sub> ×Na <sub>2</sub> O×CaO	0.033620	5.44
(K <sub>2</sub> O) <sup>3</sup>	-0.006662	-6.13	ZnO	-6.280	-5.78			

where the isokom temperatures are expressed in °C, the b-values are the model coefficients in Tables 4–6, the C-values are the glass component concentrations in mol% excluding silica, and n is the total number of glass components excluding silica.

The equations for calculating the confidence interval of the viscosity isokom predictions, considering the uncertainty of the glass composition of interest, have been described in earlier publications.<sup>(32,47-48)</sup> It must be noted, that all viscosity and error calculations in this work can be performed conveniently using a computer program connected to this study.<sup>(45)</sup>

### 3. The global viscosity model

Tables 4–6 list all coefficients and corresponding t-values for the global viscosity model. The standard

Table 5. Coefficients and t-values at  $\log(\eta/(Pas))=6.6$

Variable	Coefficient	t-value	Variable	Coefficient	t-value
Constant	939.479	-	TiO <sub>2</sub>	-2.862	-1.81
Al <sub>2</sub> O <sub>3</sub>	5.812	10.67	ZnO	-1.065	-1.98
B <sub>2</sub> O <sub>3</sub>	-4.366	-6.23	ZrO <sub>2</sub>	12.425	7.20
(B <sub>2</sub> O <sub>3</sub> ) <sup>2</sup>	-0.17367	-4.99	B <sub>2</sub> O <sub>3</sub> ×Na <sub>2</sub> O	0.32005	13.98
BaO	-3.385	-7.51	B <sub>2</sub> O <sub>3</sub> ×K <sub>2</sub> O	0.42514	16.31
CaO	-1.791	-7.64	B <sub>2</sub> O <sub>3</sub> ×Li <sub>2</sub> O	0.39626	5.61
F	-9.328	-17.11	B <sub>2</sub> O <sub>3</sub> ×CaO	-0.24066	-9.82
Fe <sub>2</sub> O <sub>3</sub>	-11.013	-8.21	Al <sub>2</sub> O <sub>3</sub> ×Na <sub>2</sub> O	0.08442	2.71
K <sub>2</sub> O	-20.659	-22.15	Al <sub>2</sub> O <sub>3</sub> ×K <sub>2</sub> O	0.48055	7.95
(K <sub>2</sub> O) <sup>2</sup>	0.58116	8.45	Na <sub>2</sub> O×K <sub>2</sub> O	0.15519	3.53
(K <sub>2</sub> O) <sup>3</sup>	-0.009370	-5.99	Na <sub>2</sub> O×Li <sub>2</sub> O	0.20781	4.37
Li <sub>2</sub> O	-25.075	-29.30	Na <sub>2</sub> O×CaO	0.09392	6.65
(Li <sub>2</sub> O) <sup>2</sup>	0.46012	16.42	K <sub>2</sub> O×Li <sub>2</sub> O	0.46938	13.40
MgO	0.930	2.88	K <sub>2</sub> O×MgO	0.26354	9.29
Na <sub>2</sub> O	-19.051	-25.01	K <sub>2</sub> O×CaO	0.47564	14.72
(Na <sub>2</sub> O) <sup>2</sup>	0.32209	8.93	MgO×CaO	-0.15553	-6.35
(Na <sub>2</sub> O) <sup>3</sup>	-0.002080	-3.59	B <sub>2</sub> O <sub>3</sub> ×Al <sub>2</sub> O <sub>3</sub> ×Na <sub>2</sub> O	-0.033573	-6.23
P <sub>2</sub> O <sub>5</sub>	14.857	2.01	Al <sub>2</sub> O <sub>3</sub> ×Na <sub>2</sub> O×CaO	-0.006780	-2.71
PbO	-8.871	-57.79	Na <sub>2</sub> O×MgO×CaO	-0.012589	-4.64
SrO	-2.191	-4			

error in a coefficient is given by the coefficient divided by its t-value. Coefficients not shown in Tables 4-6 have an insignificant influence<sup>(32,47-48)</sup> on the viscosity. In Table 7 goodness-of-fit and other related indicators<sup>(32,47-48)</sup> are displayed, and Tables 8-10 show the data-series that were systematically corrected in the model by constant offsets. The properties of large data-series are provided in Table 11. The correlation and inverse information matrices are given in Ref. 45. Residuals, e.g. in Table 7, are defined as the differences between observed and calculated values.

#### 4. Discussion

##### 4.1. Phase separation in the glass softening range

Multiple regression modelling using polynomial functions (Equation (2)) described the viscosity data well for most silicate glasses studied. At the viscosity level  $\log(\eta/(Pas))=6.6$  (~Littleton Softening Point), however, the borosilicate standard 717A<sup>(40)</sup> appeared as an outlier in the initial modelling stud-

ies. Initially, the predicted Littleton Softening Point was significantly higher than the value of 719°C given in the certificate.<sup>(40)</sup> Such unusual behaviour was not observed for any other of the six standards listed in Tables 1 and 12 at any viscosity level. It was concluded that either the standard or the mean of all other borosilicate data must be questionable. In this work it was decided to rely on the borosilicate standard 717A because it was carefully prepared and measured in several laboratories as described in the certificate;<sup>(40)</sup> phase separation was assumed to be absent. Concerning other glasses phase separation effects were considered as explained below. In addition, it was observed that some experimental data in the literature do not appear to be reliable. For example, rather doubtful borosilicate viscosity curves are reported by Akimov,<sup>(73)</sup> such as the one depicted in Figure 2. All data reported by Akimov were excluded from the calculations in this study.

The main reason why the standard 717A did not fit into initial models at  $\log(\eta/(Pas))=6.6$  is the influence of phase separation<sup>(74)</sup> on the viscosity. Figure 3

Table 6. Coefficients and t-values at  $\log(\eta/(Pas))=12.0$

Variable	Coefficient	t-value	Variable	Coefficient	t-value
Constant	624.829		PbO	-4.349	-54.42
Al <sub>2</sub> O <sub>3</sub>	4.929	16.68	SrO	1.388	4.80
B <sub>2</sub> O <sub>3</sub>	-1.121	-3.24	TiO <sub>2</sub>	3.864	18.70
BaO	-1.110	-3.75	ZrO <sub>2</sub>	8.927	4.82
CaO	6.840	20.93	B <sub>2</sub> O <sub>3</sub> ×Na <sub>2</sub> O	0.38413	18.10
(CaO) <sup>2</sup>	-0.08269	-14.07	B <sub>2</sub> O <sub>3</sub> ×CaO	-0.20958	-7.91
F	-8.123	-9.93	B <sub>2</sub> O <sub>3</sub> ×Al <sub>2</sub> O <sub>3</sub>	-0.33380	-4.55
Fe <sub>2</sub> O <sub>3</sub>	-8.453	-1.77	Al <sub>2</sub> O <sub>3</sub> ×CaO	-0.13741	-5.44
K <sub>2</sub> O	-12.460	-21.02	Na <sub>2</sub> O×K <sub>2</sub> O	0.06169	3.35
(K <sub>2</sub> O) <sup>2</sup>	0.39706	8.42	Na <sub>2</sub> O×Li <sub>2</sub> O	0.08558	5.26
(K <sub>2</sub> O) <sup>3</sup>	-0.005382	-5.05	Na <sub>2</sub> O×CaO	-0.10283	-8.56
Li <sub>2</sub> O	-11.571	-19.38	K <sub>2</sub> O×Li <sub>2</sub> O	0.17538	9.30
(Li <sub>2</sub> O) <sup>2</sup>	0.27802	7.75	K <sub>2</sub> O×MgO	0.27425	3.61
(Li <sub>2</sub> O) <sup>3</sup>	-0.002576	-4.41	K <sub>2</sub> O×CaO	0.22470	6.09
MgO	1.141	4.41	MgO×CaO	-0.21563	-8.30
Na <sub>2</sub> O	-12.854	-29.36	CaO×Li <sub>2</sub> O	-0.88170	-7.97
(Na <sub>2</sub> O) <sup>2</sup>	0.35785	15.09	Al <sub>2</sub> O <sub>3</sub> ×Na <sub>2</sub> O×CaO	0.013868	4.21
(Na <sub>2</sub> O) <sup>3</sup>	-0.004179	-10.37			

Table 7. Statistical model indicators

	log( $\eta$ /(Pa s))		
	1.5	6.6	12.0
Number of data	1090	640	597
Degree of freedom	1031	597	558
Standard model error (°C)	16.5334	9.7859	8.8174
R <sup>2</sup>	0.9894	0.9854	0.9854
R <sup>2</sup> (adjusted)	0.9888	0.9871	0.9844
R <sup>2</sup> (predicted)	0.9878	0.9116*	0.9827
R <sup>2</sup> (validation)**	0.9881	0.9812	0.9835
Standard deviation of residuals (°C)	16.09	9.46	8.53
Observation minimum (°C)	695.6	405.6	322.9
Observation maximum (°C)	1563.9	980.0	769.5
Observation average (°C)	1201.74	710.92	511.95
Observation standard deviation (°C)	156.09	86.01	70.66

\* R<sup>2</sup> (predicted) at log( $\eta$ /(Pa s))=6.6 is clearly lower than the other R<sup>2</sup> values because one statistical outlier was force-fitted into the model at log( $\eta$ /(Pa s))=6.6 as explained in the discussion. The statistical outlier was not in the 20% validation dataset by chance, therefore, R<sup>2</sup> (validation) at log( $\eta$ /(Pa s))=6.6 is rather high.

\*\* R<sup>2</sup> (validation) was calculated based on the exclusion of 20% of all data from the model, using the coefficients derived from the remaining 80%. The selection of the excluded 20% of data was performed by sorting all the data in order of increasing isokom temperature, and choosing every fifth set.

shows a viscosity curve of a borosilicate glass that has a strong tendency to phase separate below 753.5°C. At low temperatures the viscosity is much higher than it would be expected from high temperature data due to the formation of a continuous silica-rich phase<sup>(75)</sup> during cooling. Many common borosilicate glasses have a tendency towards phase separation with a continuous silica-rich phase. This tendency is not as strong as the example in Figure 3, however, because of inhibition by Al<sub>2</sub>O<sub>3</sub>, K<sub>2</sub>O, and other components such as those found in standard 717A. In commercial glasses, phase separation is also prevented kinetically through sufficiently high cooling rates.<sup>(76, p 92)</sup> Figure 4 depicts the metastable immiscibility curve in the system SiO<sub>2</sub>–Na<sub>2</sub>O–B<sub>2</sub>O<sub>3</sub>.

Phase separation in common borosilicates occurs in the glass softening range,<sup>(74–76)</sup> while at high temperatures the separated phases dissolve mutually, and at low temperatures in the glass annealing range it is inhibited kinetically or thermodynamically.<sup>(78)</sup> Borosilicate glasses that are cooled sufficiently quickly are homogeneous at low and high temperatures, while during viscosity measurement in the softening range, phase separation takes place and the viscosity

Table 8. Systematic offsets at log( $\eta$ /(Pa s))=1.5

Reference	Offset (°C)	t-value
Allison <i>et al</i> <sup>(49)</sup>	-43.09	-12.69
Eipeltauert <i>et al</i> <sup>(50)</sup>	28.54	6.78
Eipeltauert <i>et al</i> <sup>(51)</sup>	-44.83	-11.20
English <sup>(5,52)</sup>	-80.28	-10.51
Kurachi <sup>(53)</sup>	40.09	7.44
Ota <i>et al</i> <sup>(54)</sup>	-21.95	-4.61
Evstropiev <i>et al</i> <sup>(55)</sup>	20.15	3.49
Preston <sup>(56)</sup>	-24.59	-5.45
Sasek <sup>(57)</sup>	25.74	6.85
Shvaiko-Shvaikovskaya <sup>(58)</sup>	-15.13	-4.02
Tang <sup>(59)</sup>	32.65	4.75
Washburn <sup>(60)</sup>	56.15	10.52

Table 9. Systematic offsets at log( $\eta$ /(Pa s))=6.6

Reference	Offset (°C)	t-value
Allison <i>et al</i> <sup>(49)</sup>	-16.75	-8.40
Flannery <sup>(61)</sup>	-11.88	-3.78
Robinson <sup>(62)</sup>	-8.39	-2.37
Yue <sup>(63)</sup>	13.78	2.95

increases.

Hence, in this work the borosilicate standard 717A was introduced in the model at log( $\eta$ /(Pa s))=6.6 with a tenfold weight compared to all other glasses, thereby mitigating the influence of phase separation in other borosilicates. It can be concluded that softening range viscosity data of borosilicate glasses should be published carefully, only after examining the phase separation tendency through prolonged viscosity measurements under isothermal conditions, light scattering experiments, or similar measures.

#### 4.2. Evaporation loss during melting

It is a curious property of the viscosity models in this study that most data series show a trend, as depicted in Figure 5, that to the best of the author's knowledge cannot simply be traced back to a linear influence of any published glass component or component combination. The data series in Figure 5 from Lakatos *et al*,<sup>(7)</sup> Hrma *et al*,<sup>(38)</sup> and the Owens-Illinois Company<sup>(67)</sup> are important because glass engineers and scientist frequently use them for viscosity modelling. Trends similar to those in Figure 5 are not limited to soda–lime–silica glasses, but also can be observed in other glass families such as most borosilicates, TV panel compositions, and lead silicates. The average of all residual trends of individual data series in this work is 0.09, i.e. in a series spanning over 200°C the residuals increase 18°C in going from low to high temperature isokoms. The residual trend of all data series combined in the three models of this study is insignificant, the trends apply to the individual series only.

Residual trends, as seen in Figure 5, also appear if all coefficients representing component interactions and offsets in the tables are excluded, according to the well known linear additivity principle,<sup>(1,34–37)</sup> The trends are also present in very simple viscosity models, such as that given by considering all binary SiO<sub>2</sub>–Na<sub>2</sub>O glasses in SciGlass,<sup>(1)</sup> or sometimes even in viscosity additivity models for one single series, e.g. the soda–lime–silica container glasses in the 'High temperature glass melt property database'.<sup>(38,65–66)</sup> It can be stated that residual trends as observed in

Table 10. Systematic offsets at log( $\eta$ /(Pa s))=12.0

Reference	Offset (°C)	t-value
Allison <i>et al</i> <sup>(49)</sup>	-8.30	-4.49
Nemilov <sup>(64)</sup>	-7.01	-3.96
Robinson <sup>(62)</sup>	-8.61	-2.61
Shelby <sup>(65)</sup>	5.87	4.39

Table 11. Properties of large data series (- residual, - standard deviation, avg. - average, # of data excluding outliers, corr. - mathematically corrected to zero)

Reference	# of data	log( $\eta/((Pa s))$ )	$\Delta$ avg. (°C)	$\sigma$ (°C) of residuals	Glass type / system
Hrma <i>et al</i> <sup>(38)</sup>	122	1.5	-2.0	20.0	Soda-lime-silica, TV panel, various commercial borosilicates
Fluegel <i>et al</i> <sup>(66)</sup>	140	6.6	-0.2	9.0	Soda-lime-silica, TV panel, various commercial borosilicates
Shelby <sup>(65)</sup>	131	12.0	corr.	8.5	Soda-lime-silica, TV panel, various commercial borosilicates
Owens-Illinois <sup>(67)</sup>	98	1.5	0.3	13.6	Soda-lime-silica with various additions
	102	6.6	0.3	6.2	Soda-lime-silica with various additions
Lakatos <i>et al</i> <sup>(7)</sup>	72	1.5	1.8	11.4	Soda-lime-silica, lead crystal, borosilicates
	30	6.6	2.3	4.0	Soda-lime-silica, lead crystal, borosilicates
	30	12.0	1.7	3.3	Soda-lime-silica, lead crystal, borosilicates
Allison <i>et al</i> <sup>(49)</sup>	28	1.5	corr.	13.5	Soda-lime-silica with small additions of boron oxide
	28	6.6	corr.	5.2	Soda-lime-silica with small additions of boron oxide
	28	12.0	corr.	4.7	Soda-lime-silica with small additions of boron oxide
Eipeltaufer <i>et al</i> <sup>(50,51)</sup>	49	1.5	corr.	18.3	Binary sodium and potassium silicates
Liska <sup>(68)</sup>	35	1.5	1.0	17.2	Soda-lime-silica plus TiO <sub>2</sub> , ZrO <sub>2</sub>
Skorniyakov <sup>(69)</sup>	32	1.5	-1.8	13.0	Soda lead silicates
Owens <sup>(70)</sup>	40	1.5	3.2	15.2	R-glasses (high CaO, Al <sub>2</sub> O <sub>3</sub> , no B <sub>2</sub> O <sub>3</sub> )
Various authors <sup>(25,71)</sup>	217	1.5	-0.7	14.4	Glasses for nuclear waste immobilization
Nemilow <i>et al</i> <sup>(64)</sup>	24	6.6	-1.0	13.6	Lead silica, alkali silicates
	48	12.0	corr.	7.8	Lead silica, alkali silicates
Poole <i>et al</i> <sup>(72)</sup>	63	12.0	0.4	7.4	Alkali silicates, soda-lime-silica
Shvaiko-Shvaikovskaya <sup>(58)</sup>	24	1.5	corr.	18.6	Soda-lime-silica
	19	6.6	0.5	5.4	Soda-lime-silica
	21	12.0	-2.9	6.2	Soda-lime-silica

Figure 5 are not caused by the statistical analysis. Naturally, residual trends in models developed from only one data series are often relatively insignificant because the trends are interpreted as compositional effects. Therefore, the errors of such local models sometimes appear small, which may not necessarily reflect the reality.

The residual trends cannot be reduced to a viscosity curve that does not follow the VFT Equation (1) or non-Newtonian viscous flow because the calculations in this work are not based on any such assumptions. It also cannot be concluded that thermocouple or viscometer calibrations are systematically incorrect, as such influences cannot be detected in the viscosity models presented here. Furthermore, it is not possible to link the trends to changing glass chemistry with increasing temperature because this effect is accounted for already, evidenced by the fact that no overall trends can be observed in the models; the trends appear only in individual series. Instead, an attempt was made to investigate the relation between alkali and boron oxide evaporation and the residual trends. To achieve this an additional variable was introduced into the models representing the product of the isokom temperature in °C and the sum of the volatile oxide concentrations in mol% of Na<sub>2</sub>O, K<sub>2</sub>O,

and B<sub>2</sub>O<sub>3</sub>. If the product is high, alkali and boron oxide evaporation can be expected to be more significant. Possible evaporation losses of SO<sub>3</sub>, F, NaCl, H<sub>2</sub>O, ZnO, and PbO were not taken into account.

It turned out that through consideration of evaporation with a single variable the standard model errors as seen in Table 7 can be reduced by about 15%. The fact that the evaporation variable is so significant at all of the three viscosity levels shows that evaporation mainly takes place during the glass melting process. Also quenching of the melt in water as practiced by Lakatos *et al*<sup>(7)</sup> reduces the alkali and boron oxide content. Meerlender<sup>(43)</sup> reports a relatively insignificant viscosity isokom increase of 1°C at 700°C if the completely melted standard DGG I (soda-lime-silica glass) is heat treated for 15 h at 1300-1400°C or for 20 h at 1200-1300°C under otherwise unknown conditions. The evaporation loss during glass melting is more significant than after completion of the melting process because of the high surface area of the batch and gas and water evolution. Boron oxide readily evaporates in wet furnace atmospheres.<sup>(79)</sup> In addition, the 'loss on ignition,' used to quantify surface adsorbed water in the batch materials, is not always evaluated in literature data. However, the reported chemical analysis of the

Table 12. Agreement between viscosity standards and model predictions

Standards	Isokom temperatures (°C) at viscosity level in log( $\eta/((Pa s))$ )					
	1.5		6.6		12.0	
	experiment	model	experiment	model	experiment	model
710A <sup>(39)</sup>	1319	1314	731	729	545	551
717A <sup>(40)</sup>	1388	1378	719	731	514	520
711 <sup>(41)</sup>	1185	1172	614	614	443	445
710 <sup>(42)</sup>	1293	1294	725	732	556	564
DGG I <sup>(43)</sup>	1301	1303	721	715	539	535
WGS <sup>(44)</sup>	947	947	565	(538)*	457	(418)*

\* The glass composition is outside the model validity limits.

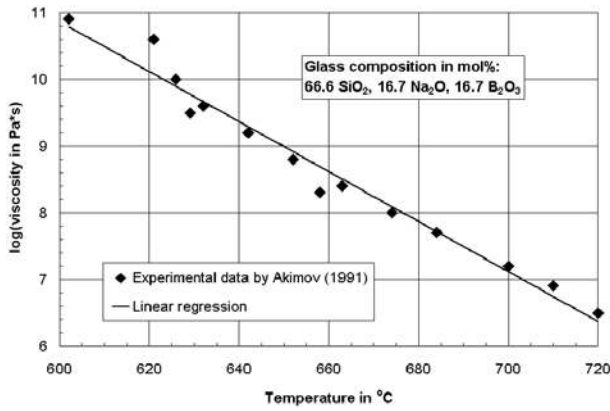


Figure 2. Viscosity data reported by Akimov (1991)<sup>(73)</sup>

glass compositions in some large data series<sup>(7,38,49,65-67)</sup> theoretically should account for evaporation losses, especially if the chemical analysis was performed not before<sup>(38,65-66)</sup> but after high-temperature viscosity measurements.<sup>(7)</sup> This work did not detect that the chemical analysis has an influence on the composition-viscosity relation because an accurate chemical analysis of multicomponent silicate glasses is more difficult than viscosity measurements. For verification, the batched and analysed compositions of hundreds of borosilicate glasses for nuclear waste vitrification.<sup>(25,71)</sup> were compared. It turned out that the average error (standard deviation of differences between batched and analysed concentrations) of the Na<sub>2</sub>O concentrations for 687 waste glasses containing an average of 13.4 wt% Na<sub>2</sub>O was 10.2% of the total Na<sub>2</sub>O content, with an evaporation loss of 3.2% of the total Na<sub>2</sub>O content. Concerning B<sub>2</sub>O<sub>3</sub> the error was 8.0% of the total B<sub>2</sub>O<sub>3</sub> content of 9.6 wt%, with an evaporation loss of 0.7% of the total B<sub>2</sub>O<sub>3</sub> content.

As seen in the aforementioned example, evaporation losses during glass melting are difficult to detect by chemical analysis. According to gravimetric investigations by the author on simplified compositions an evaporative loss of about 3% of the total Na<sub>2</sub>O content is reasonable in laboratory experiments. Assuming evaporative losses similar to those seen with waste

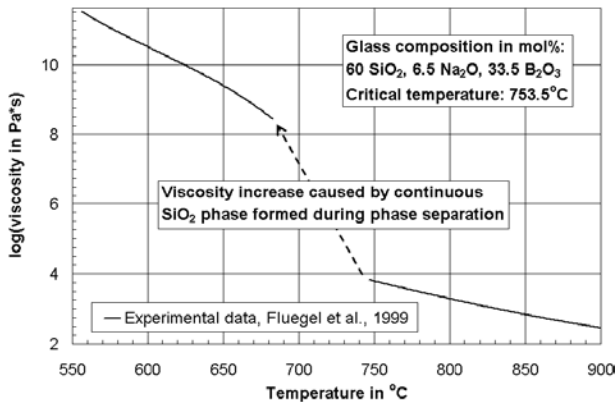


Figure 3. Viscosity increase caused by phase separation during cooling<sup>(75)</sup>

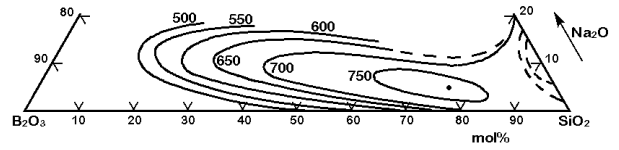


Figure 4. Metastable phase separation in the system SiO<sub>2</sub>-Na<sub>2</sub>O-B<sub>2</sub>O<sub>3</sub>, temperatures (°C), concentrations in mol%<sup>(74,77)</sup>

glasses, viscosity isokom temperatures for an average composition in this work would increase by about 9°C at log(η/(Pa·s))=1.5, 4°C at log(η/(Pa·s))=6.6, and 2°C at log(η/(Pa·s))=12.0, which is not sufficient to fully account for the observed residual trends.

The introduction of an evaporation variable for Na<sub>2</sub>O, K<sub>2</sub>O, and B<sub>2</sub>O<sub>3</sub> reduces the residual trends such as those seen in Figure 5, but it does not remove them. Either there exist other factors that influence the composition-viscosity relation at high temperatures within the measurement series, or the evaporative loss was not represented correctly by the simple variable employed in this study. Evaporation does not increase linearly with temperature as assumed for simplicity here, but exponentially. Furthermore, it is possible that the different batch materials used in each of the various studies have slightly different

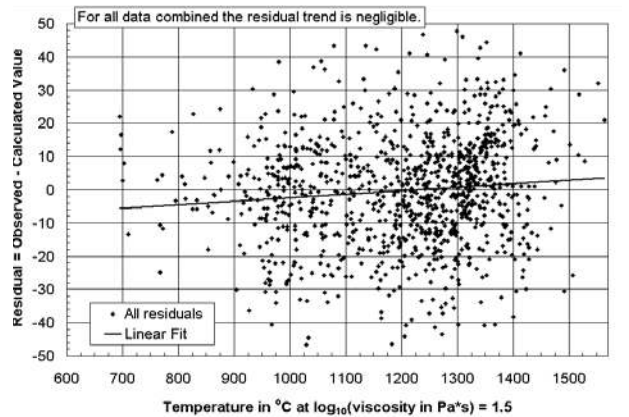
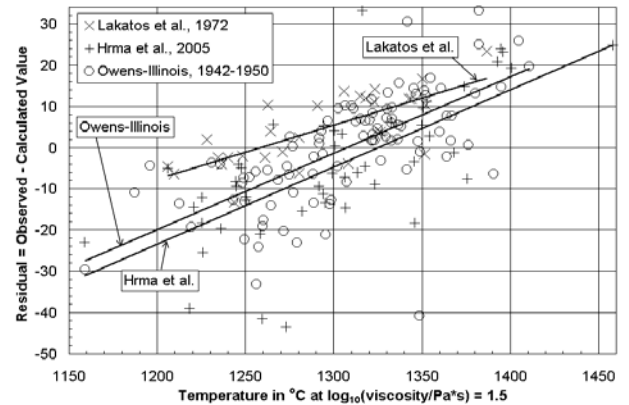


Figure 5. Residual trends in °C at glass melting temperatures (The data in the diagram by Hrma et al consider only soda-lime-silica container and float glasses to maintain readability)



compositions which are difficult to analyse in the resulting glass, for example they may contain differing amounts of physically adsorbed water. In laboratory experiments of the author often the melted glass is about 1 wt% lighter than the batch composition suggests, even considering  $\text{Na}_2\text{O}$  and  $\text{B}_2\text{O}_3$  evaporation. Varying water content in the batch materials would result in a different water contents in the resulting glasses; the water content would be expected to decrease with increasing melting temperature and time. Also the melting conditions, for example is the melting atmosphere wet or dry, can have similar influences on the glass composition.

In this paper, variables taking into account evaporation and the water content were not introduced in the final model versions presented in Tables 4–6 because further experimental investigations and modelling work are recommended first. It is suggested that glasses with high viscosity, high concentrations of volatile compounds, and based on this work high residuals, should be studied. In addition, a statistical analysis dedicated to the glass water content should be performed, if possible, augmented by selected experiments. Through a few verification experiments the prediction errors of the model could be reduced significantly.

The residual trends are part of the cause (besides component interactions) of viscosity models based on a single data series being poor at predicting the viscosities for other data series, especially if the glasses in the other series include another area of temperature-viscosity behaviour.

### 4.3. Model accuracy

Besides the phase separation effects mentioned above, glasses within specific composition areas were not identified as outlier suspects; i.e. sharp composition–viscosity trends did not seem to exist that could not be described through polynomial functions. The glass composition–viscosity relation appears to show a smooth behaviour. Further phase separation or crystallisation effects did not occur. It is possible that sharp composition–viscosity trends within the limits of validity of the model described in this work<sup>(45)</sup> might be discovered in future.

This study enables predictions of the viscosity isotherms temperatures of silicate glasses with a standard error of 9–17°C based on over 100 references given in SciGlass<sup>(1)</sup> and the Tables 1, and 8–11. The degrees of freedom<sup>(32,47–48)</sup> in Table 7 are very close to the total number of the analysed data. There are about 15 times more data in the models than variables, which makes them equivalent to a one-variable linear regression using 15 data points. With one exception the models do not contain data points with high leverage<sup>(32,47–48)</sup> as demonstrated by  $R^2$  (predicted) and  $R^2$  (valida-

tion) in Table 7. One experimental value of a binary potassium silicate glass (30 mol%  $\text{K}_2\text{O}^{(80)}$ ) with high leverage and large residual was force fitted into the model at  $\log(\eta/(\text{Pas}))=6.6$  because the data point appeared reasonable compared to other data in the composition area based on knowledge of the subject matter.

The similarity between  $R^2$  and  $R^2$ (adjusted) in Table 8 shows that the models are not over-fitted with too many variables.

The experimental errors derived from fitting all the data for binary alkali silicate glasses listed in SciGlass<sup>(1)</sup> are close to the standard model errors in Table 7, which is an indicator that the model is not over- or under-fitted. The model appears to have the same accuracy as the experimental measurements.

A comparison of hundreds of experimental data with the model predictions from this work is given in Table 11. It is not surprising that the majority of the experimental data agree well with the model because the model is based directly on the experimental findings, without intermediate assumptions about the glass structure (formation of chemical equilibria between structural groups) or property relations (between viscosity and heat capacity, Gibbs free energy difference of devitrification, enthalpy of melting, thermal expansion, liquidus temperature, surface tension, molar volume, shear modulus, cooling rate), such as in the models by Conradt<sup>(22)</sup> or Priven.<sup>(28)</sup> On the contrary, structural group formations and property relations can be recognised to their full extent only after a statistical analysis of the available data, such an analysis has been initiated in this study.

The advantage of the empirical modelling approach is its high accuracy, when the limits of validity of the model are considered.

Numerous viscosity models due to other authors exist.<sup>(7–33)</sup> The global model developed in this study is more versatile and accurate than previous works, as demonstrated in Table 2. This is caused by the fact that the source data of most previous models plus additional published values were combined in this paper through advanced statistical analysis. Outside the limits of validity of this study,<sup>(45)</sup> other models can be used.<sup>(22,28–29)</sup>

An experimental model validation would be superior to the data splitting and  $R^2$  (predicted) calculation procedures used in this work. At present, it is not possible to compare model predictions to findings of other investigators because the model includes all of them. Further experimental investigations are required.

The data series in Tables 8–10 do not compare well to findings of other investigators. The offsets of those series are assumed to indicate systematic measurement errors that had to be corrected mathematically in this work. The error in the series by Allison *et al.*<sup>(49)</sup>

has been reported previously.<sup>(31)</sup> Some systematic errors such as those in the work of Eipeltaufer *et al.*<sup>(51)</sup> can be confirmed by analysing data in binary glass systems only. The correlation matrices<sup>(45)</sup> indicate that the systematic offsets of the series in Tables 8–10 are not strongly correlated with other model variables, which means that the offsets cannot be explained by unique glass composition regions investigated in those series. However, weak correlations remain. Further experimental investigations can help improving the accuracy of the systematic offsets.

Data series without systematic offsets in Tables 8–10 and with a low standard deviation,  $\sigma$ , of the residuals in Table 11 were regarded as being of high quality (high precision), for example the series reported by the Owens-Illinois Company<sup>(67)</sup> or Lakatos *et al.*<sup>(7)</sup> The incorporation of those data series in this study decreases the error of the model and makes high accuracy predictions possible. In contrast, series with high  $\sigma$  of the residuals increase the error.

It cannot be claimed that all the composition-viscosity trends found in Tables 4–6 or rejected as insignificant are of the same accuracy. However, within the limits of validity of the model<sup>(45)</sup> all composition-viscosity trends fall within the confidence interval for the predictions.<sup>(45)</sup>

The certified values of six viscosity standards agree well with the predictions of the model listed in Table 12. It needs to be considered that not all viscosity levels and chemical compositions of the standards are certified.

Based on all of the statements above it is claimed that the viscosity models in Table 4–6 are accurate, including error calculations derived from the inverse information matrix<sup>(48)</sup> in Ref. 45. Viscosity isokom temperatures values of glasses that fall into the application ranges of this work given in Ref. 45, and with a residual larger than three times the model standard errors in Table 7 might be questionable. Previously published viscosity models cannot claim the same level of accuracy as this study because they are based on experimental data from only one or a few selected laboratories as explained in the introduction, and therefore are missing systematic inter-laboratory comparison.

#### 4.4. Influence of the glass composition on the viscosity

All single component coefficients  $b_i$  from Equation (2) in the Tables 4–6 have the unit °C/mol%, and they quantify the viscosity isokom variation caused by the exchange of 1 mol% SiO<sub>2</sub> by 1 mol% of the considered component. For example, if 1 mol% fluoride ions are introduced into a silicate glass in exchange for 1 mol% SiO<sub>2</sub>, the temperature of constant viscosity (isokom) at  $\log(\eta/(\text{Pa s}))=1.5$  decreases by 11.7°C, while at

higher viscosities the isokom temperature decreases by 9.3 and 8.1°C, respectively.

Because the main component SiO<sub>2</sub> was excluded from the calculation following the slack variable modelling approach,<sup>(32,47–48)</sup> all coefficients represent interactions with SiO<sub>2</sub>.

For an accurate interpretation of model coefficients, the correlation matrices given in Ref. 45 must be considered. Unfortunately, none of the variables are absolutely statistically independent; i.e. all variables interfere more or less mutually. It is believed that in the immediate future, it will not be possible to decorrelate all variables completely because this would require a high number of well planned and very accurate measurements. Therefore, it is recommended to consider the model coefficients in this paper as preliminary findings until further experimental data become available. Nevertheless, as long as all validity limits summarised in Ref. 45 are followed, accurate predictions are possible.

Because of mutual correlations, it is suggested that the predictions of the model are compared rather than coefficient values to evaluate the influences of various glass components on the viscosity for a specific practical application, such as in the examples in Figures 1, 6 to 14, and 16.

The model constants  $b_i$  in Tables 4–6 theoretically are supposed to represent the viscosity isokom temperatures of glasses comprising mainly SiO<sub>2</sub>, and all components with insignificant influence on the viscosity such as H<sub>2</sub>O, some fining and colouring agents, and impurities. However, few experimental data exist for high silica glasses, and the models in this paper are not applicable to those composition areas.

Influences of the glass composition on the viscosity can be extracted from Tables 4–6. General trends are discussed in other publications.<sup>(31–32,34 (p 128,156))</sup> Figures 6 to 12 display spider graphs calculated using the model for approximate average compositions at the investigated viscosity levels. In Figure 6 at high temperature the composition-viscosity functions (excluding the one for B<sub>2</sub>O<sub>3</sub>) appear to be rather linear, while at lower temperatures in Figures 9 and 11 more curvature is observed. It can be concluded that the component interactions, which cause deviations from additive linear composition-property relations, are especially strong at low temperatures. At high temperatures thermal dissociation reduces many interactions. Another common tendency is that most glass components decrease the viscosity at high temperatures, while at low temperatures significantly fewer components have a viscosity lowering effect.

##### 4.4.1. Silica

SiO<sub>2</sub> always increases the viscosity in common silicate glasses, especially at high temperatures. At low tem-

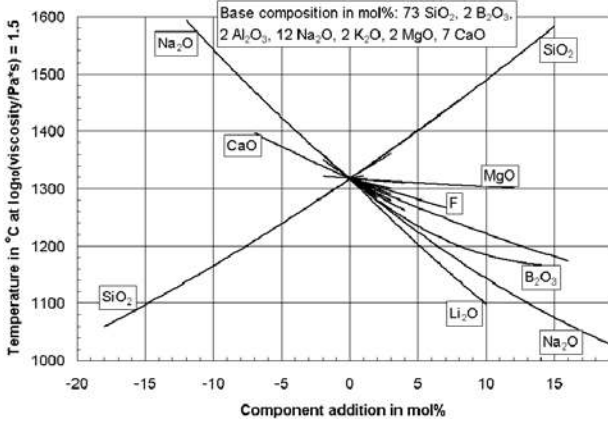


Figure 6. Spider-graph for the given specific base composition using the model at  $\log(\eta/(\text{Pa}\cdot\text{s}))=1.5$ ; the spider-graph is different for other base compositions. For any component addition the ratios of all the remaining components remain constant

peratures other components can increase the viscosity more than silica as seen in Figures 11 and 12.

#### 4.4.2. Boron oxide

$\text{B}_2\text{O}_3$  strongly decreases the viscosity at high temperatures, while at low temperatures this influence is reversed. The coefficients in Tables 4–6 assume that boron oxide on its own always decreases the viscosity, however, in interaction with sodium oxide a strong viscosity increase occurs, which is a manifestation of the boron oxide anomaly.<sup>(34(p138),76(p138))</sup> In Figure 13 it is demonstrated how the viscosity isokom temperatures in ternary sodium borosilicate glasses increase upon replacement of silica by boron oxide. The boron oxide anomaly involving  $\text{Li}_2\text{O}$  and  $\text{K}_2\text{O}$  is not represented in the model in Table 6 at  $\log(\eta/(\text{Pa}\cdot\text{s}))=12.0$  because limited experimental data for common potassium and lithium borosilicate glasses are available. However, from the model at the viscosity level  $\log(\eta/(\text{Pa}\cdot\text{s}))=6.6$  (Table 5) it can be concluded that  $\text{Li}_2\text{O}$ ,  $\text{Na}_2\text{O}$ , and  $\text{K}_2\text{O}$  show comparable influences of the boron oxide

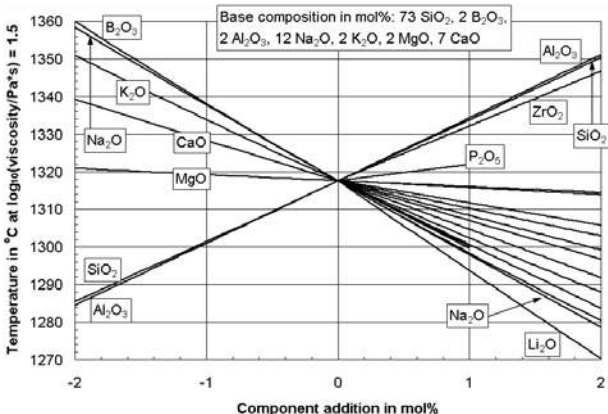


Figure 7. Magnification of Figure 6; spider-graph at  $\log(\eta/(\text{Pa}\cdot\text{s}))=1.5$

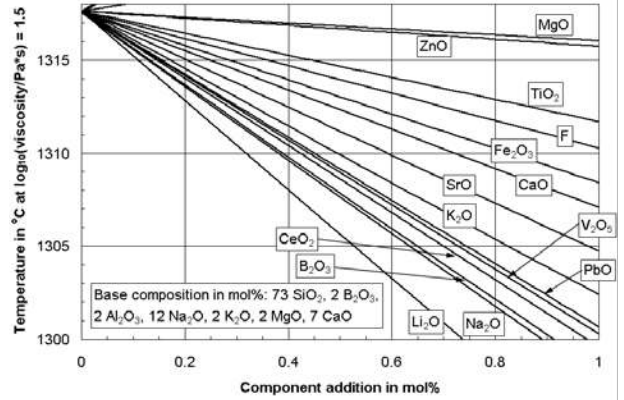


Figure 8. Magnification of Figure 7, spider-graph at  $\log(\eta/(\text{Pa}\cdot\text{s}))=1.5$ ; polyvalent oxidation states other than those shown in the figure must be converted to the given oxides on a molar basis. The 95% confidence interval of the model mean in Figure 8 is 3–8°C, depending on the glass composition

anomaly.

With increasing temperature the boron oxide anomaly decreases as reported in the literature<sup>(61)</sup> and comprehensible through application of the model considered in this study. Therefore, boron oxide tends to shorten the temperature–viscosity curve of soda–lime–silica glasses.

#### 4.4.3. Phosphorus oxide

$\text{P}_2\text{O}_5$  increases the viscosity of silicate glasses as shown in Figure 7, and the coefficients in Table 5. The not-mentioned (insignificant) coefficient in Table 4 shows that  $\text{P}_2\text{O}_5$  does not change the viscosity isokom at  $\log(\eta/(\text{Pa}\cdot\text{s}))=1.5$  if introduced into a glass in exchange for silica; i.e. it increases the viscosity isokom to a similar extent to silica. Especially at low temperatures  $\text{P}_2\text{O}_5$  can cause phase separation and

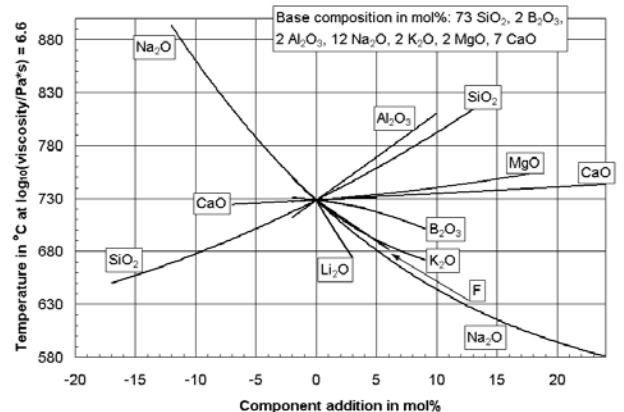


Figure 9. Spider-graph for the given specific base composition using the model at  $\log(\eta/(\text{Pa}\cdot\text{s}))=6.6$  (~Littleton Softening Point); The spider-graph is different for other base compositions. For any component addition the ratios of all the remaining components remain constant

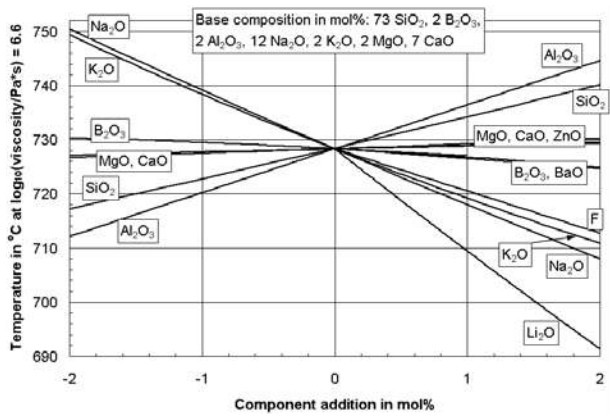


Figure 10. Magnification of Figure 9; spider-graph at  $\log(\eta/(\text{Pa}\cdot\text{s}))=6.6$  (~Littleton Softening Point)

crystallisation<sup>(76 (p 92))</sup> that may significantly alter the viscosity.

#### 4.4.4. Alumina and other intermediate glass oxides

Al<sub>2</sub>O<sub>3</sub> strongly increases the viscosity of commercial glasses, most significantly at low temperatures, caused by the elimination of nonbridging oxygen sites. ZrO<sub>2</sub> shows a very similar influence on the viscosity. Other intermediate glass oxides like TiO<sub>2</sub> or ZnO increase the viscosity at low temperatures or have no influence respectively, while at high temperatures the viscosity is decreased. Some heavy oxides such as PbO or Bi<sub>2</sub>O<sub>3</sub> have a strong viscosity lowering effect over the full temperature range because of their high cation polarisability. Further intermediate oxide influences can be derived from the coefficients in Tables 4–6. In particular the model at  $\log(\eta/(\text{Pa}\cdot\text{s}))=1.5$  given in Table 4 contains a large number of intermediate glass oxides as the source

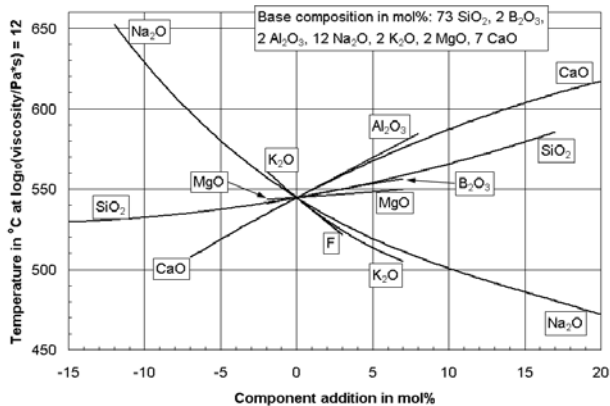


Figure 11. Spider-graph for the given specific base composition using the model at  $\log(\eta/(\text{Pa}\cdot\text{s}))=12.0$ ; The spider-graph is different for other base compositions. For any component addition the ratios of all the remaining components remain constant

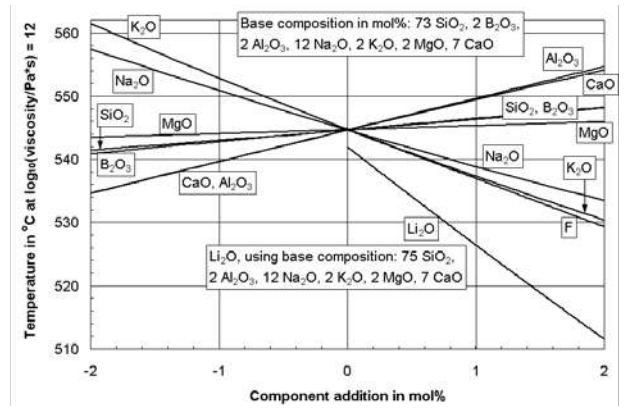


Figure 12. Magnification of Figure 11, spider-graph at  $\log(\eta/(\text{Pa}\cdot\text{s}))=12.0$ ; to demonstrate the influence of Li<sub>2</sub>O this graph is based on a slightly different base composition to previous figures because of the limits of validity of the model

data including multicomponent glasses for nuclear waste immobilisation.<sup>(25,71)</sup>

#### 4.4.5. Alkali and alkaline earth oxides

Alkali and alkaline earth oxides are traditional glass network modifiers that lead to the formation of non-bridging oxygen sites. They all decrease the viscosity in the glass melting range approximately in the order MgO<CaO<SrO<BaO<K<sub>2</sub>O<Na<sub>2</sub>O<Li<sub>2</sub>O (strongest effect). The order may slightly change depending on the glass composition. Various effects seem to interfere because, interestingly, alkaline earth oxides with high atomic weight often decrease the viscosity more than alkaline earth oxides with low atomic weight, but for alkali oxides this trend is reversed. The alkaline earth oxides possess the ability to bridge over two non-bridging oxygen sites at low temperature, thereby strengthening the network and increasing the viscosity. MgO can show special properties because of its partial glass forming abilities at high alkali concentrations.<sup>(34(p134))</sup>

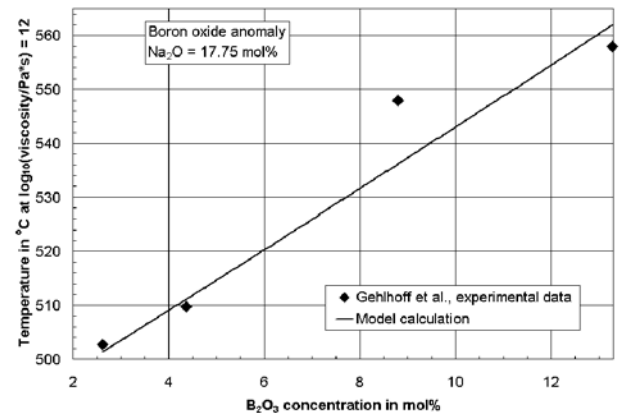


Figure 13. Comparison of viscosity increase based on boron oxide anomaly in the ternary system SiO<sub>2</sub>-B<sub>2</sub>O<sub>3</sub>-Na<sub>2</sub>O at  $\log(\eta/(\text{Pa}\cdot\text{s}))=12.0$  after Gehlhoff & Thomas<sup>(6)</sup> and the model in this work

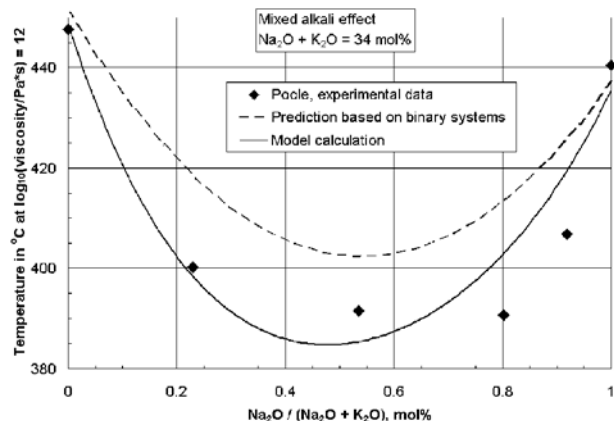


Figure 14. Comparison of the viscosity decrease caused by the mixed-alkali effect in the ternary system  $\text{SiO}_2\text{--Na}_2\text{O--K}_2\text{O}$  at  $\log(\eta/(\text{Pa s}))=12.0$  after Poole<sup>(72)</sup> and the models in this work

It is interesting to note that in binary alkali silicates, according to the original data<sup>(1)</sup> and the model in Table 6 at the viscosity level  $\log(\eta/(\text{Pa s}))=12.0$ ,  $\text{Li}_2\text{O}$  surprisingly does not decrease the viscosity isokoms as much as  $\text{Na}_2\text{O}$ . However, in multicomponent glasses  $\text{Li}_2\text{O}$  has the stronger effect (see Figure 12), again in agreement with the experimental data in SciGlass.<sup>(1)</sup> It is possible that phase separation and crystallisation in binary lithium silicates<sup>(82–83)</sup> are the cause of this behaviour.

One of the most widely studied component interactions in glasses is the mixed alkali effect,<sup>(84–86,34 (p 132))</sup> especially for properties based on diffusivity such as the electrical conductivity. Controversy exists to the present day about the origin of this effect. The mixed alkali effect also influences the viscosity. Figure 14 illustrates the observation that at a constant total alkali concentration ternary mixed alkali silicate glasses have a lower viscosity than either of the two corresponding binary alkali silicates. This effect can be observed most distinctly at low temperatures, while in the glass melting range its influence is significantly reduced. The mixed alkali effect is the cause of the stronger influence of  $\text{K}_2\text{O}$  as compared to  $\text{Na}_2\text{O}$  on the viscosity isokom temperatures in Figures 11 and 12. As the viscosity at low temperatures is significantly reduced, and at the same time at high temperatures not much change occurs, the mixed alkali effect extends the glass working range. The mixed alkali effect for viscosity may also be observed at low total alkali concentrations, as opposed to that for the electrical conductivity. For example, Leko<sup>(87)</sup> found a deep minimum of the viscosity isokom temperatures at  $\log(\eta/(\text{Pa s}))=10$  in ternary mixed alkali glasses containing 5 mol%  $\text{Na}_2\text{O}+\text{K}_2\text{O}$  total, when there was no mixed alkali effect for the electrical conductivity. In contrast, Nemilov<sup>(88)</sup> did not observe a mixed alkali effect for the viscosity in ternary sodium potassium silicates below 10 mol% total alkali content.

The mixed alkali effect has a negative (decreasing) effect on viscosity isokom temperatures. The model predictions in this study describe this behaviour well, as demonstrated by Figures 14, 11, and 12. Therefore, it is all the more surprising that all mixed alkali coefficients  $\text{Na}_2\text{O}\times\text{K}_2\text{O}$ ,  $\text{Na}_2\text{O}\times\text{Li}_2\text{O}$ , and  $\text{K}_2\text{O}\times\text{Li}_2\text{O}$  in Tables 4–6 are not negative, but positive. This cannot be explained by linear variable correlation effects,<sup>(32,47–48)</sup> because the correlation matrix<sup>(45)</sup> shows that all noteworthy correlations are positive and reduce the values of the mixed alkali coefficients  $\text{Na}_2\text{O}\times\text{K}_2\text{O}$ ,  $\text{Na}_2\text{O}\times\text{Li}_2\text{O}$ , and  $\text{K}_2\text{O}\times\text{Li}_2\text{O}$ .

During the common model fitting technique applied here<sup>(32,47–48)</sup> all coefficients are optimised to yield the simplest result with the maximum  $R^2$  value. An examination of the coefficients in Tables 4–6 shows that the mixed alkali effect is not obtained through the coefficients  $\text{Na}_2\text{O}\times\text{K}_2\text{O}$ ,  $\text{Na}_2\text{O}\times\text{Li}_2\text{O}$ , and  $\text{K}_2\text{O}\times\text{Li}_2\text{O}$ , but rather through the coefficients  $\text{Na}_2\text{O}$ ,  $(\text{Na}_2\text{O})^2$ ,  $(\text{Na}_2\text{O})^3$ ,  $\text{K}_2\text{O}$ ,  $(\text{K}_2\text{O})^2$ ,  $(\text{K}_2\text{O})^3$ ,  $\text{Li}_2\text{O}$ ,  $(\text{Li}_2\text{O})^2$ , and  $(\text{Li}_2\text{O})^3$ , based largely on experimental data from independent binary alkali silicate systems. The model describes the viscosity behaviour in binary alkali silicates and ternary mixed alkali silicates equally well, using mainly the coefficients for binary alkali silicates. Therefore, following the logic of the model the mixed alkali effect for the viscosity is not caused by alkali–alkali interactions in the first place but mainly by independent alkali–silica interactions. Alkali–silica interactions cause small additions of alkali oxide to pure silica glass to have a relative stronger influence on the viscosity than large additions. In other words, the mixed alkali effect is a manifestation of a general nonlinear composition–viscosity behaviour, well known in binary alkali silicate glasses.

For additional confirmation of this statement a simple model was developed, based exclusively on all available composition–viscosity data for the binary systems  $\text{SiO}_2\text{--Na}_2\text{O}$  and  $\text{SiO}_2\text{--K}_2\text{O}$  given in the SciGlass databases<sup>(1)</sup> listed in Tables 13 and 14. The derived model is given in Table 15, and the dotted line in Figure 14 shows its application to the mixed-alkali system studied by Poole.<sup>(72)</sup> It is obvious in Figure 14 that a mixed alkali effect for the viscosity derives directly from nonlinear composition–viscosity behaviour of independent binary systems, without alkali–alkali interaction.

Figure 15 shows the nonlinear composition–viscosity behaviour in binary glasses in one of its extreme cases. The experimental data in Figure 15 were published by Leko *et al.*,<sup>(1,89)</sup> and they are well accepted based on comparable values<sup>(34 (p 165))</sup> and the structural model by Avramov *et al.*<sup>(90)</sup> The models in this paper cannot be applied to the high silica glasses shown in Figure 15; however, in Figure 1 and Tables 13 and 14 it is also shown that at higher alkali concentrations the composition–viscosity curves in the binary systems

Table 13. Viscosity isokom (*v.i.*) temperatures (°C) at  $\log(\eta/(\text{Pa s}))=12.0$  in the binary system  $\text{SiO}_2\text{--Na}_2\text{O}$  from SciGlass,<sup>(1)</sup> concentrations in mol%

Ref.	Na <sub>2</sub> O	<i>v.i.</i>	Ref.	Na <sub>2</sub> O	<i>v.i.</i>	Ref.	Na <sub>2</sub> O	<i>v.i.</i>
54	33.3	430.0	58	20.0	470.7	92	33.4	457.1
55	34.0	433.9		25.0	461.0	93	30.0	462.1
	33.8	443.5		30.0	455.0		19.8	465.3
	35.5	445.0		35.0	444.4		17.2	476.6
	37.1	428.1		40.0	419.8	64	20.0	472.8
	32.0	449.0	5	24.8	477.8		13.0	578.0
94	23.1	461.1	95	33.3	441.6		20.0	473.0
	27.6	456.0		50.0	415.7	72	14.7	503.8
96	15.0	553.4	97	40.0	431.3		20.1	475.7
	20.0	498.8	98	15.5	530.9		24.8	464.6
	25.0	463.9		16.9	482.5		34.5	440.5
	33.0	447.2		22.8	459.7		39.5	407.6
	40.0	405.2		33.6	434.7	99	17.5	474.0
	42.0	399.0	100	33.0	464.1		28.5	484.1
101	39.3	427.3		15.0	499.9		33.3	457.0
102	34.5	421.0	6	17.5	470.0		41.0	405.1
103	34.0	439.6	104	25.0	454.6		30.3	463.0
105	20.0	484.4	106	17.1	486.7	63	26.0	471.7
	30.0	462.2		19.6	479.2	107	25.0	460.7
108	25.0	448.1						

$\text{SiO}_2\text{--Na}_2\text{O}$  and  $\text{SiO}_2\text{--K}_2\text{O}$  are nonlinear. Additional examples of nonlinear composition–property behaviour have been provided by Mazurin *et al.*<sup>(91)</sup> using the SciGlass database.<sup>(1)</sup>

The positive coefficients for  $\text{Na}_2\text{O}\times\text{K}_2\text{O}$ ,  $\text{Na}_2\text{O}\times\text{Li}_2\text{O}$ , and  $\text{K}_2\text{O}\times\text{Li}_2\text{O}$  could be caused by interactions between two different alkali oxide–silica bonding structures, which have a comparatively *weak* influence on the viscosity. On the other hand, the mixed alkali effect for viscosity is largely based on interactions between alkali oxides and silica, which have a comparatively *strong* influence on the viscosity, without direct alkali–alkali interference. Alkali ion interactions in mixed alkali glasses through ion pair formation cannot be conclusively verified experimentally,<sup>(109)</sup> which means the modelling efforts of Lyon, which assume a theoretical mixed alkali compound  $\text{Na}_2\text{K}_2\text{O}_2$  in glass, appear unreliable.<sup>(14)</sup> The fact that mixed alkali glasses produced at temperatures below  $T_g$  by ion exchange sometimes show a mixed alkali effect for the electrical conductivity<sup>(110)</sup> and sometimes do not<sup>(111)</sup> underscores the importance of interaction with the major network former that mainly occurs during heating of those ion exchanged glasses above  $T_g$ .

Table 14. Viscosity isokom (*v.i.*) temperatures (°C) at  $\log(\eta/(\text{Pa s}))=12.0$  in the binary system  $\text{SiO}_2\text{--K}_2\text{O}$  from SciGlass,<sup>(1)</sup> concentrations (mol%)

Ref.	K <sub>2</sub> O	<i>v.i.</i>	Ref.	K <sub>2</sub> O	<i>v.i.</i>
64	30.0	448.4	72	8.0	554.9
	13.0	517.5		10.6	519.6
	20.0	490.7		18.0	495.9
	30.0	448.0		18.5	498.2
	13.0	517.0		24.5	477.1
	20.0	491.0		29.2	454.8
105	20.0	492.0		34.1	447.6
54	33.3	471.6			
	33.3*	490.0*			

\* This value may be considered an outlier.

Table 15. Model based on data from the binary systems  $\text{SiO}_2\text{--Na}_2\text{O}$  and  $\text{SiO}_2\text{--K}_2\text{O}$  in Tables 13 and 14

Variable	Coefficient	t-value
Constant	596.911	-
Na <sub>2</sub> O	-6.801	-5.45
(Na <sub>2</sub> O) <sub>2</sub>	0.061754	2.82
K <sub>2</sub> O	-7.070	-3.92
(K <sub>2</sub> O) <sub>2</sub>	0.081970	1.85
R <sub>2</sub>	0.8056	
Standard model error (°C)	15.6558	

According to the model, the mixed alkali effect for viscosity is not a special case that occurs exclusively in mixed alkali silicate glasses. Many glass components show nonlinear composition–viscosity trends. The literature reports mixed alkaline earth<sup>(112)</sup> (see also Figure 16), mixed oxide,<sup>(110,113)</sup> mixed anion,<sup>(114)</sup> mixed alkali–water,<sup>(115)</sup> and mixed glass former<sup>(116)</sup> effects that even occur in glasses where nonbridging oxygen sites are absent.<sup>(117)</sup> In addition, mixed mobile ion,<sup>(118)</sup> and similar effects<sup>(86,119)</sup> are known for other properties and quite possibly also occur for viscosity. Naturally, the mixing effects can only be observed as viscosity minima or maxima as long as the influences of the considered components are similar; otherwise, the strong difference between both influences leads to a more or less nonlinear composition–viscosity function without extrema if mixing effects are present.

From the  $\text{MgO}\times\text{CaO}$  coefficients in Tables 4–6 it appears that the simultaneous presence of MgO and CaO in a glass decreases viscosity isokoms, especially at low temperatures. It is likely that the negative  $\text{MgO}\times\text{CaO}$  coefficients are a manifestation of a mixed alkaline earth effect that could not be reduced otherwise to MgO and CaO squared and cubic terms, based mainly on binary alkaline earth silicates, because those glasses are difficult or impossible to prepare.

The models in this study do not explain the cause of the mixed alkali effect for the viscosity and similar composition–viscosity trends, but they show that the mixed alkali effect and nonlinear composi-

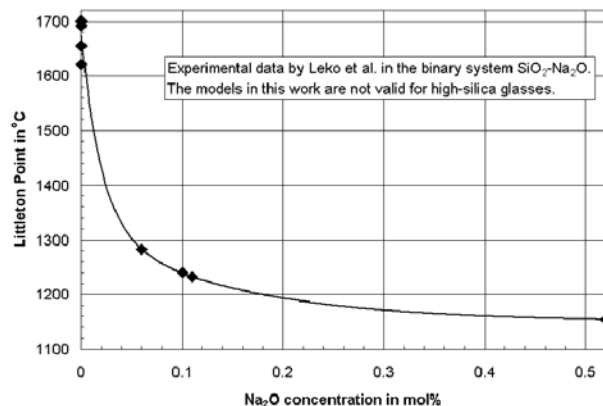


Figure 15. Isokom temperature at  $\log(\eta/(\text{Pa s}))=6.6$  (~Littleton softening point) in the binary glass system  $\text{SiO}_2\text{--Na}_2\text{O}$  after Leko *et al.*<sup>(89)</sup>

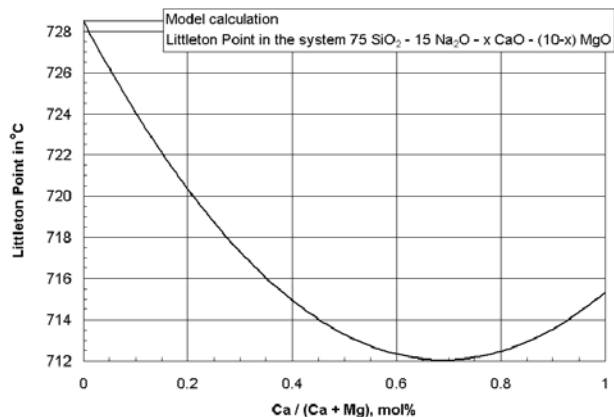


Figure 16. Model calculation of the isokom temperature at  $\log(\eta/(Pa s))=6.6$  (~Littleton softening point) in the glass system  $SiO_2-Na_2O-CaO-MgO$ . The 95% confidence interval of the model mean in Figure 16 is 2–6 °C, depending on the glass composition

tion–viscosity trends in binary glasses largely have the same origin, namely interactions of individual alkali oxides with glass network formers rather than interactions between alkali oxides. Details of those network former–alkali interactions remain the topic for other research such as that of Avramov *et al.*<sup>(90)</sup> especially with regards to such extreme behaviour as that seen in Figure 15.

If this hypothesis concerning the mixed alkali effect for the viscosity holds true, it should *not* vanish at low alkali concentrations because at low alkali concentrations the composition–viscosity behaviour becomes strongly nonlinear as seen in Figure 15. This is in agreement with experimental observations on silicate glasses made by Leko<sup>(87)</sup> who observed the mixed alkali effect at 5 mol% total alkali content, and in disagreement with observations by Nemilov<sup>(88)</sup> who did not observe it at 10 mol% total alkali content.

It would be interesting to apply the approach presented here to the mixed alkali effects of other properties, especially the electrical conductivity. For this purpose it needs to be considered that the mixed alkali effect must have at least two causes with opposite influence. If only one cause existed (glass network weakening) then with decreasing viscosity the conductivity would increase when alkalis are mixed. However, the mixed alkali effect leads to a decrease of the electrical conductivity (ion mobility reduction). Glass network weakening by itself leads to an improved ion mobility. This contradiction is recognised but not often discussed or even understood in the literature<sup>(84,p260)</sup> because the main focus of mixed alkali research is centred on the electrical conductivity, i.e. the reduction in ion mobility. With respect to viscosity the mixed alkali effect appears to be mainly due to the mixing of two independent binary systems, in the case of the electrical conductivity strong alkali–alkali interactions need to be taken

into account. This agrees in principle with Kim *et al.*<sup>(120)</sup> who conclude from their experiments that the mixed alkali effects for viscosity and electrical conductivity must be considered separately. It is possible that the  $Na_2O \times K_2O$ ,  $Na_2O \times Li_2O$ , and  $K_2O \times Li_2O$  interactions in Tables 4–6, that moderately increase the viscosity, have a strong impeding effect on the alkali ion mobility. If proven correct, those opposing causes might be the reason why the mixed alkali effect for the electrical conductivity is not observed at low alkali concentrations; i.e. network weakening and reduction in ion mobility due to alkali–alkali interactions cancel each other as far as ion mobility is concerned. In this respect it is beneficial to evaluate the experimental findings of Ivanov,<sup>(121)</sup> according to which the conductivity minimum in mixed alkali germanate glasses not only disappears at low alkali concentrations into a linear function, but beyond this, the curvature slightly reverses from concave to convex. Accordingly, at very low alkali concentrations it could be speculated that the mixed alkali effect for electrical conductivity may reverse if the influence of the network weakening on the ion mobility is stronger than the reduction in ion mobility caused by alkali–alkali interactions.

#### 4.4.6. Anions and water

Fluoride and chloride ions in glass lower the viscosity because of the creation of terminal Si–F and Si–Cl bonds. Polar molecules such as H<sub>2</sub>O lower the viscosity as well, based on dissociation and reaction with Si–O bonds. The influence of water could not be detected in this work because of the few available data and the difficulty of H<sub>2</sub>O analysis in glass.<sup>(122)</sup> However, the viscosity lowering effect of H<sub>2</sub>O is well known in the literature.<sup>(34(p145),115,123)</sup> Also sulfur oxides and associated anions, expressed commonly as SO<sub>3</sub>, decrease the viscosity of glass melts, while in the glass transition and softening range no influence could be detected because of the few available data.

## 5. Conclusions

Models based on multiple regression using polynomial functions for estimating the temperature–viscosity behaviour of silicate glasses from their chemical composition have been developed. The models combine the majority of the published data relevant to commercial glass production and the previous models derived from them in unified equations. The accuracy of prediction could be improved through an advanced statistical analysis approach, for example by analysing systematic differences between laboratories. Detailed error calculations for the predictions are possible, considering the uncertainty of the chemical glass composition of interest.<sup>(45)</sup> The

accuracy of prediction is comparable to measurement series performed in several laboratories, and it is superior to the accuracy of a single measurement.

The presented models provide a new approach to the mixed alkali effect. It has been shown that the mixed alkali effect for viscosity is largely not caused by alkali–alkali interactions, but rather by nonlinear alkali–silica interactions. The mixed alkali effect for viscosity is not limited to mixed alkali glasses or alkali oxides, but can occur in any other system where nonlinear composition–viscosity behaviour is observed.

Evaporation losses during glass melting have been demonstrated to influence the viscosity significantly.

### Acknowledgements

I would like to thank Oleg V. Mazurin, St. Petersburg, Russia, for providing a large number of viscosity data from the SciGlass information system.

### References

1. SciGlass 6.5 Database and Information System, 2005. [www.sciglass.info](http://www.sciglass.info)
2. Vogel, H. Temperaturabhängigkeitsgesetz der Viskosität von Flüssigkeiten (Law of Temperature Dependence of Liquids). *Phys. Zeitschrift*, 1921, **22**, 645–6. (In German.)
3. Fulcher, G. S. Analysis of recent measurements of the viscosity of glasses. *J. Am. Ceram. Soc.*, 1925, **8** (6), 339–55.
4. Tammann, G. & Hesse, W. Die abhängigkeit der viskosität von der temperatur bei unterkühlten flüssigkeiten (Dependence of the viscosity from the temperature in undercooled liquids). *Zeitschrift für Anorganische und Allgemeine Chemie*, 1926, **156**, 245–57.
5. English, S. The effect of composition on the viscosity of glass. *J. Soc. Glass Technol.*, 1924, **8**, 205–48; 1925, **9**, 83–98; 1926, **10**, 52–66.
6. Gehlhoff, G. & Thomas, M. Thomas; *Zeit. Techn. Phys.*, 1925, **6**, 544; 1926, **7**, 105; 1926, **7**, 260–78. (In German.)
7. Lakatos, T., Johansson, L.-G. & Simmingsköld, B. *Glass Technol.* 1972, **13** (3), 88–95; *Glastekn. Tidskr.*, 1972, **27** (2), 25–8; *Glastekn. Tidskr.*, 1973, **28**, 75–9; *Glastekn. Tidskr.*, 1975, **30** (1), 7–8; *Glastekn. Tidskr.*, 1976, **31**, 31–5; *Glastekn. Tidskr.*, 1976, **31**, 51–4; *Glastekn. Tidskr.*, 1977, **32** (2), 31–5; *Glastekn. Tidskr.*, 1978, **33** (3), 55–9; *Glastekn. Tidskr.*, 1979, **34**, 61–5.
8. Okhotin, M. V. *Stek. Keram. Promyshlennost*, 1947, **3**, 12; *Steklo Keram.*, 1954, **1**, 7.
9. Mazurin, O. V., Tretiakova, N. I. & Shvaiko-Shvaikovskaya, T. P. Metod rascheta viazkosti silikatnykh stekol. Deposited in VINITI, 1969, no. DEP1091-69.
10. Sasek, L., Meissnerova, H. & Kovandova, J. Application of mathematical-statistical methods in silicate research. Part 6. Determinations of mathematical relations for the calculation of the temperature dependence of viscosity in the range of  $\eta=10^{17}$ – $10^{14}$  and  $\eta=10^2$ – $10^{14}$  d(Pa s) from chemical composition of the glass. (Orig. Czech); *Sb. Vys. Sk. Chem.-Technol. Praze, Chem. Technol. Silik.* 1977, **L7**, 149–218.
11. Braginskii, K. I. Calculation of the viscosity of glass as a function of temperature. *Glass Ceram.*, 1973, **30**, 451–4.
12. Rodriguez Cuartas, R. Calculo teorico de propiedades del vidrio: viscosidad, parametros termicos y parametros de desvitrificacion. (Theoretical calculation of glass properties: viscosity, thermic parameters and parameters of devitrification. *Ceram. Vidr.*, 1984, **23**, 105–11.
13. Ledererova, V., Smrcek, A. & Rysavy, J. Faktoren zur berechnung von eigenschaften von kalk-natrongläsern. (Factors for the calculation of properties of soda-lime glasses. (Orig. Czech); *Sklar Keram.*, 1986, **36**, 304–8.
14. Lyon, K. C. Prediction of the viscosities of soda-lime-silica glasses. *J. Res. Nat. Bur. Standards A*, 1974, **78A** (4), 497–504.
15. Bottinga, Y. & Weill, D. F. The viscosity of magmatic silicate liquids:

- a model for calculation. *Am. J. Sci.*, 1972, **272**, 438–75.
16. Herbert, J., Prod'homme, M. & Derobert, M. Viscosity-temperature relations in the  $\text{SiO}_2$ - $\text{Na}_2\text{O}$ - $\text{K}_2\text{O}$ - $\text{Al}_2\text{O}_3$ - $\text{B}_2\text{O}_3$ - $\text{PbO}$  system in the composition range of lead crystal glass. *Verres Refract.*, 1976, **30** (2), 219–21.
17. Leko, V. K. *Fiz. Khim. Stekla*, 1980, **6** (5), 553; *Fiz. Khim. Stekla*, 1982, **8** (2); Leko, V. K. & Mazurin, O. V. *Svoistva Kvoartsevoogo Stekla*. Leningrad, 1985.
18. Urbain, G., Cambier, F., Deletter, M. & Anseau, M. R. Viscosity of silicate melts. *Trans. J. Br. Ceram. Soc.*, 1981, **80** (4), 139–41.
19. Belousov, Yu. L. & Firsov, V. A. *Fiz. Khim. Stekla*, 1991, **17** (3), 411.
20. Belousov, Yu. L. & Akulova, M. V. *Fiz. Khim. Stekla*, 1992, **18** (4), 94; Pushkareva, M. V. Printsipy i metod rascheta vyazkosti stekol v shirokom intervale sostavov i temperatur. Thesis, Belgorod, 1993.
21. Kozuykov, V. M. & Mazurin, O. V. *Fiz. Khim. Stekla*, 1994, **20** (4), 449.
22. Conradt, R. Thermodynamic approach to viscosity in the glass transition. *Glastech. Ber., Glass Sci. Technol.*, 1994, **67** (11), 304–11.
23. Öksoy, D., Pye, D. L. & Boulos, E. N. Statistical analysis of viscosity-composition data in glassmaking. *Glastech. Ber., Glass Sci. Technol.*, 1994, **67** (7), 189–95.
24. Kozuykov, V. M. & Mazurin, O. V. Calculation of viscosity of sodium-calcium silicate melts. *Fiz. Khim. Stekla*, 1994, **20** (4), 449–60. (In Russian.)
25. Hrma, P. R., Piepel, G. F. et al. *Property/composition relationships for Hanford high-level waste glasses melting at 1150°C*. PNL Report 10359 to the US Department of Energy, 1994, 1–2; Vienna, J. D. & Hrma, P. R. et al. Effect of composition and temperature on the properties of high level waste (HLW) glass melting above 1200°C (Draft); PNNL Report 10987 to the US Department of Energy, 1996. Hrma, P. & Robertus, R. J. Waste glass design based on property composition functions. *Ceram. Eng. Sci. Proc.*, 1993, **14** (11/12), 187–203; Hrma, P., Piepel, G. F., Redgate, P. E., Smith, D. E., Schweiger, M. J., Vienna, J. D. & Kim, D. S. Prediction of processing properties for nuclear waste glasses. *Ceram. Trans.*, **61**, 505–13.
26. Björkvall, J., Du Sichen, Stolyarova, V. & Seetharaman, S. A model description of the thermochemical properties of multicomponent slags and its application to slag viscosities. *Glass Phys. Chem.*, 2001, **27** (2), 132–47.
27. Korsgaard, M., Pind, M., Moller, P., Sorensen, S. & Woldum, H. S. Derivation of the temperature dependent constants for  $\text{KAlO}_2$  and  $\text{NaAlO}_2$  in a viscosity predictive model for high aluminosilicate melts. *Glass Sci. Technol.*, 2003, **76** (6), 270–4.
28. Priven, A. I. General method for calculating the properties of oxide glasses and glass-forming melts from their composition and temperature. *Glass Technol.*, 2004, **45** (6), 244–54. Priven, A. I. Calculation of the viscosity of glass-forming melts. Part 1. The  $\text{Li}_2\text{O}$ - $\text{Na}_2\text{O}$ - $\text{K}_2\text{O}$ - $\text{SiO}_2$  system. *Glass Phys. Chem.*, 1997, **23** (5), 344–53. Priven, A. I. Calculation of the viscosity of glass-forming melts. Part 2. The  $\text{MgO}$ - $\text{CaO}$ - $\text{SrO}$ - $\text{BaO}$ - $\text{Al}_2\text{O}_3$ - $\text{SiO}_2$  system. *Glass Phys. Chem.*, 1997, **23** (6), 416–28. Priven, A. I. Calculation of the viscosity of glass-forming melts. Part 3. The  $\text{Al}_2\text{O}_3$ - $\text{RO}$ - $\text{Al}_2\text{O}_3$ - $\text{SiO}_2$  system. *Glass Phys. Chem.*, 1998, **24** (1), 19–30. Priven, A. I. Calculation of the viscosity of glass-forming melts. Part 4. A unified method for calculating the viscosity of silicate and aluminate melts. *Glass Phys. Chem.*, 1998, **24** (1), 31–40. Priven, A. I. Calculation of the viscosity of glass-forming melts. Part 5. Binary borate Systems. *Glass Phys. Chem.*, 2000, **26** (6), 541–58. Priven, A. I. Calculation of the viscosity of glass-forming Melts. Part 6. The  $\text{R}_2\text{O}$ - $\text{B}_2\text{O}_3$ - $\text{SiO}_2$  and  $\text{RO}$ - $\text{B}_2\text{O}_3$ - $\text{SiO}_2$  ternary borosilicate systems. *Glass Phys. Chem.*, 2001, **27** (4), 360–70. Priven, A. I. Calculation of the temperature coefficient of viscosity logarithm  $\partial \log \eta / \partial \log T$  for oxide melts in the glass transition range from their composition. *Glass Phys. Chem.*, 2000, **26** (5), 455–69. Priven, A. I. Comparative characterisation of methods for calculating the viscosity of silicate glass-forming melts. *Glass Phys. Chem.*, 1997, **23** (5), 333–43. Priven, A. I. A new equation for describing the temperature dependence of the viscosity of glass-forming melts. *Glass Phys. Chem.*, 1999, **25** (6), 491–7. Priven, A. I. Calculation of temperature dependences of the viscosity and volume relaxation time for oxide glass-forming melts from chemical composition and dilatometric glass transition temperature. *Glass Phys. Chem.*, 2001, **27** (6), 527–42.
29. Russell, J. K. & Giordano, D. A model for silicate melt viscosity in the system  $\text{CaMgSi}_2\text{O}_6$ - $\text{CaAl}_2\text{Si}_2\text{O}_8$ - $\text{NaAlSi}_3\text{O}_8$ . *Geochim. Cosmochim. Acta*, 2005, **69** (22), 5333–49.
30. Fluegel, A., Varshneya, A. K., Seward, T. P. & Earl, D. A. Viscosity of commercial glasses in the softening range. *Proc. Seventh Int. Conf. on Advances in Fusion and Processing of Glass III*. Edited by J. R. Varner, T. P. Seward, H. Schaeffer, The American Ceramic Society, Westerville,



- Ohio, USA. *Ceram. Trans.*, 2004, 141, 379–86.
31. Fluegel, A., Varshneya, A. K., Earl, D. A., Seward, T. P. & Oksoy, D. Improved composition-property relations in silicate glasses. Part 1. Viscosity. *Ceram. Trans.*, 2005, 170, 129–43.
  32. Fluegel, A., Earl, D. A., Varshneya, A. K. & Oksoy, D. Statistical analysis of viscosity, electrical resistivity, and further glass melt properties. *High temperature glass melt property database for process modelling*. Edited by T. P. Seward III & T. Vascott; The American Ceramic Society, Westerville, Ohio, 2005, Chapter 9.
  33. Hrma, P. High-temperature viscosity of commercial glass. *Ceram. Silikaty*, 2006, 50 (2), 57–66.
  34. Scholze, H. *Glass - nature, structure and properties*. Springer-Verlag, 1991, ISBN 0-387-97396-6.
  35. Volf, M. B. Mathematical approach to glass. *Glass Sci. Technol.*, 1988, 9.
  36. Martlew, D. Viscosity of molten glasses. *Properties of Glass-Forming Melts*. Edited by L. D. Pye, A. Montenegro, I. Joseph, CRC Press, Boca Raton, Florida, 2005, Chapter 5.
  37. International Glass Database System INTERGLAD Ver.6; New Glass Forum, Tokyo, Japan.
  38. Hrma, P., See, C. A., Lam, O. P. & Minister, K. B. C. High-temperature viscosity of commercial glasses. *High temperature glass melt property database for process modelling*. Edited by T. P. Seward III & T. Vascott; The American Ceramic Society, Westerville, Ohio, 2005, Chapter 7.
  39. *Standard Reference Material 710A, Soda-Lime-Silica Glass*. National Institute of Standards & Technology (NIST), Gaithersburg, MD, 20899, USA, March 20, 1991.
  40. *Standard Reference Material 717A, Borosilicate Glass*. National Institute of Standards & Technology (NIST), Gaithersburg, MD, 20899, USA; September 18, 1996.
  41. *Standard Sample No. 711, Certificate of Viscosity Values, Lead-Silica Glass*. National Bureau of Standards, U.S. Department of Commerce, Washington, D.C., 20235, USA; July 1, 1964.
  42. Napolitano, A. & Hawkins, E. G. Viscosity of a standard soda-lime-silica glass. *J. Res. Nat. Bur. Stand. A.*, 1964, 68A (5), 439–48.
  43. Meerlender, G. Viskositäts-Temperaturverhalten des Standardglases I der DGG (DGG - Deutsche Glastechnische Gesellschaft, German Society of Glass Technology). *Glastechn. Ber.*, 1974, 47 (1), 1–3.
  44. Waste Glass Standard, personal communication, publication in preparation. The Waste Glass Standard was established in Round-Robin tests with several participating laboratories.
  45. Viscosity calculation program, model validity limits, inverse information and correlation matrices available at <http://glassproperties.com/viscosity/>
  46. Shelby, J. E. *High temperature glass melt property database for process modelling*. Edited by T. P. Seward III and T. Vascott, The American Ceramic Society, Westerville, Ohio, 2005, Appendix I.
  47. Fluegel, A., Earl, D. A., Varshneya, A. K. & Seward, T. P. Density and thermal expansion calculation of silicate glass melts. *Proc. CD 79th Glastechnische Tagung*, Wuerzburg, Germany, 23–25 May 2005.
  48. Fluegel, A. Statistical regression modelling of glass properties - a tutorial. *Glass Technol., Eur. J. Glass Sci. Technol. A*, in press.
  49. Allison, R. S. & Turner, W. E. S. Further investigations upon the influence of boric oxide on the rate of melting of the batch, and on the rate of refining and of setting of commercial glasses of the soda-lime-silica type. *J. Soc. Glass Technol.*, 1954, 38, 297–364.
  50. Eipeltauer, E. & More, A. *Radex-Rundschn.*, 1960, 4, 230.
  51. Eipeltauer, E. & Jangg, G. *Kolloid Zh.*, 1955, 142 (2–3), 77.
  52. English, S. & Turner, W. E. S. *J. Soc. Glass Technol.*, 1921, 5, 121–3; *J. Soc. Glass Technol.*, 1928, 12, 75–81; Turner, W. E. S. & Winks, F. *J. Soc. Glass Technol.*, 1928, 12, 57–74.
  53. Data by J. Kurachi (2003) from the SciGlass Database. Private communication, O. V. Mazurin.
  54. Ota, R. & Fukunaga, J. *Advances in Fusion of Glass*. American Ceramic Society, Westerville, Ohio, 1988, 31; Ota, R. & Fukunaga, J. *Proc. XVth Int. Congr. on Glass*. Leningrad, 1989, 1a, 162; Ota, R., Tsuchiya, F., Kawamura, K., Nakanishi, Sh. & Fukunaga, J. *J. Ceram. Soc. Jpn.*, 1991, 99 (2), 168.
  55. Evstropiev, K. S. & Pospelov, B. A. *Fiziko-Khimicheskie Svoistva Troinoi Sistemy Na<sub>2</sub>O–PbO–SiO<sub>2</sub>*. Moskva, 1949, 70. (In Russian.)
  56. Preston, E. Viscosity of soda-silica glasses at high temperatures and its bearing on their constitution. *J. Soc. Glass Technol.*, 1938, 22, 45–81.
  57. Sasek, L., Meissnerova, H. & Hoffmann, O. *Sb. Vys. Sk. Chem. Technol. Praze, Chem. Technol. Silik.*, 1975, L6, 153; Sasek, L., Meissnerova, H. & Persin, J. *Sb. Vys. Sk. Chem. Technol. Praze, Chem. Technol. Silik.*, 1973, L4, 87; Sasek, L., Meissnerova, H. & Hozkova, V. *Sb. Vys. Sk. Chem. Technol. Praze, Chem. Technol. Silik.*, 1975, L6, 131; Sasek, L., Mika, M. & Rada, M. *Silikaty*, 1988, 32 (3), 209; Mika, M. & Piepel, G. F. *Ceram. Silikaty*, 1997, 41 (4), 141; Sasek, L. *Silikaty*, 1963, 7 (4), 270.
  58. Shvaiko-Shvaikovskaya, T. P., Mazurin, O. V. & Bashun, Z. S. *Neorg. Mater.*, 1971, 7 (1), 143; Shvaiko-Shvaikovskaya, T. P., *Steklo*, 1968, 3, 93; Shvaiko-Shvaikovskaya, T. P., Gusakova, N. K. & Mazurin, O. V. *Neorg. Mater.*, 1971, 7 (4), 713; Shvaiko-Shvaikovskaya, T. P., Gusakova, N. K. & Mazurin, O. V. *Vyazkost Stekol Sistemy Na<sub>2</sub>O–CaO–SiO<sub>2</sub> v Shyrokom Intervale Temperatur*. Deposited in VINITI, Moscow, No. 483–71 Dep., 1971.
  59. Tang, Y. & Frischat, G. H. *Glustech. Ber.*, 1990, 63K, 410; Tang, Y. & Frischat, G. H. Influence of small additions of Li<sub>2</sub>O raw materials on glass melting. *Glustech. Ber., Glass Sci. Technol.*, 1995, 68 (7), 213.
  60. Washburn, E. W., Shelton, G. R. & Libman, E. E. *Univ. Ill. Bull.*, 1924, 21 (S140), 33.
  61. Flannery, J. E., Morgan, D. W., Rosplock, S. E. & Sczerbaniewicz, S. A. US Patent No. 4273586 Cl 3 C 03 C 3/04, *Off. Gazette*, 1981, 1007 (3).
  62. Robinson, H. A. & Peterson, C. A. Viscosity of recent container glass. *J. Am. Ceram. Soc.*, 1944, 27 (5), 129–38.
  63. Yue Y. & Brueckner, R. Influence of homologous substitutions of chemical components on the rheological properties and on isochomal workability of silicate glass melts. *Glustech. Ber., Glass Sci. Technol.*, 1996, 69 (7), 204–15; Yue, Y. & Bruckner, R. *Glustech. Ber., Glass Sci. Technol.*, 1996, 69 (10), 311.
  64. Nemilov, S. V. & Ignatjev, A. I. *Fiz. Khim. Stekla*, 1990, 16 (1), 85; Nemilov, S. V. *Neorg. Mater.*, 1968, 4 (6), 952; Nemilov, S. V. *Zh. Prikl. Khim.*, 1969, 42 (1), 55.
  65. Shelby, J. E. Transformation range viscosity measurements. *High temperature glass melt property database for process modelling*. Edited by T. P. Seward III & T. Vascott, The American Ceramic Society, Westerville, Ohio (2005), Chapter 7.
  66. Fluegel, A. & Varshneya, A. K. Parallel plate viscometry. *High temperature glass melt property database for process modelling*. Edited by T. P. Seward III & T. Vascott, The American Ceramic Society, Westerville, Ohio (2005), Chapter 7.
  67. Owens-Illinois Glass Company, General Research Laboratory. Effect of barium oxide and zinc oxide on the properties of soda-dolomite lime-silica glass. *J. Am. Ceram. Soc.*, 1942, 25 (3), 61–9; Effect of iron oxide on the properties of soda-dolomite lime-silica glass. *J. Am. Ceram. Soc.*, 1942, 25 (14), 401–8; Effect of substituting MgO for CaO on properties of typical soda-lime glasses. *J. Am. Ceram. Soc.*, 1944, 27 (8), 221–5; Effect of fluorine and phosphorus pentoxide on properties of soda-dolomite lime-silica glass. *J. Am. Ceram. Soc.*, 1944, 27 (12), 369–72; Properties of soda-strontium oxide-alumina-silica glasses. *J. Am. Ceram. Soc.*, 1948, 31 (1), 1–8; Effect of boric oxide on properties of soda-dolomite lime-silica glass. *J. Am. Ceram. Soc.*, 1948, 31 (1), p 8–14; Effect of K<sub>2</sub>O and Li<sub>2</sub>O on properties of soda-dolomite lime-silica glasses. *J. Am. Ceram. Soc.*, 1950, 33, 181–6.
  68. M. Liska, P. Simurka. “Viscosity of the glass forming melts in the 15Na<sub>2</sub>O, 10(MgO, CaO, TiO<sub>2</sub>, ZrO<sub>2</sub>), 75SiO<sub>2</sub> system. *Phys. Chem. Glasses*, 1995, 36 (1), 6–11; Liska, M., Klyuek, V. P., Antalík, J. & Stubna, I. Thermomodulometry and structural relaxation of Na<sub>2</sub>O\*2SiO<sub>2</sub>-Na<sub>2</sub>O\*2TiO<sub>2</sub> glasses, *Ceram. Silikaty*, 1996, 40 (3), 85–91; Liska, M., Klyuev, V. P., Antalík, J. & Stubna, I. Viscosity of Na<sub>2</sub>O\*2(TiO<sub>2</sub>, SiO<sub>2</sub>) glasses. *Phys. Chem. Glasses*, 1997, 38 (1), 6–10.
  69. Skorniyakov, M. M. *Fiziko-Khimicheskie Svoistva Troinoi Sistemy Na<sub>2</sub>O–PbO–SiO<sub>2</sub>*. Moskva, 1949, 39.
  70. Erickson, T. D. & Wolf, W. W. US Patent No. 3847626 Cl C 03 C 13/00, *Off. Gazette*, 1974, 928 (2). Owens-Corning Fiberglas Corp., GB Patent No. 1391384 Cl 2 C 03 C 13/00, 3/04, *Abridg. Specif.*, 1975, No. 4491.
  71. Bulkye & Vienna; *Plutonium Vitrification*, 1997, personal communication; Feng *et al.*, 1996, Hanford LLW Glass Formulation, personal communication; McPherson, D. *et al.* *The influence of waste variability on the properties and phase stability of the West Valley reference glass*. September 1986; Muller, I. S., Buechele, A. C. & Pegg, I. L. *Glass formulation and testing with RPP-WTP LAW simulants*. VSL-01R3560-2, 2001; Muller, I. S. & Pegg, I. L. *Glass formulation and testing with TWRS LAW simulants*. January 1998; Olson, K. M. *Fabrication and leaching of West Valley demonstration project glasses: ten quarter 2 and ten quarter 3 glasses*. October 1993; Olson, K. M. *Viscosity testing of 30 WVDP glasses*. February 1994; Staples, B. A., Scholes, B. A., Peeler, D. K., Torres, L. L., Vienna, J. D., Musick, C. A. & Boyle, B. R. *The preparation and characterisation of INTEC HAW phase 1 composition variation study glasses*. INEEL/EXT-98-00970, March 1999; Staples, B. A., Scholes, B. A., Peeler, D. K., Torres, L. L., Vienna, J. D., Musick, C. A. & Boyle, B. R. *The preparation and characterisation of INTEC phase 2b composition variation study glasses*. INEEL/EXT-99-01322, February 2000. Vienna,

- J. D. et al. 2002, *SBW Melter Glass Formulation*, personal communication.
72. Poole, J. P. & Gensamer, M. Systematic study of effect of oxide constituents on viscosity of silicate glasses at annealing temperatures. *J. Am. Ceram. Soc.*, 1949, **32** (7), 220–9; Poole, J. P. Low-temperature viscosity of alkali silicate glasses. *J. Am. Ceram. Soc.*, 1949, **32** (7), 230–3.
73. Akimov, V. V. Viscosity of sodium borosilicate glasses in the glass transition range. *The Sov. J. Glass Phys. Chem., (Fiz. Khim. Stekla)* 1991, **17** (4), 348; (5), 425.
74. *Phase separation in glass*. Edited by O. V. Mazurin & E. A. Porai-Koshits, Elsevier Science Publishers B. V., North-Holland; Amsterdam, New York, 1984.
75. Fluegel, A. *Untersuchungen zur Herstellung von Porengröße-Gradienten in Kieselglas auf der Grundlage entmischerter Natriumborosilikat-Gläser (Pore Size Gradients in Silica based on Phase-Separated Sodium Borosilicate Glasses)*. Dissertation, Jena, Germany, 1999. (In German.); Fluegel, A. & Ruessel, C. Kinetics of phase separation in a  $6.5\text{Na}_2\text{O}-33.5\text{B}_2\text{O}_3-60\text{SiO}_2$  glass. *Glass Sci. Technol.*, 2000, **73** (3), 73–8.
76. Vogel, W. *Glass Chemistry*. Springer-Verlag, 1994, Second Edition.
77. Haller, W., Blackburn, D. H., Wagstaff, F. E. & Charles, R. J. Metastable immiscibility surface in the system  $\text{Na}_2\text{O}-\text{B}_2\text{O}_3-\text{SiO}_2$ . *J. Am. Ceram. Soc.*, 1970, **53**, 34–9.
78. Polyakova, I. G. The regularities of the metastable immiscibility in the  $\text{Na}_2\text{O}-\text{B}_2\text{O}_3-\text{SiO}_2$  system: lower and upper temperature boundaries. *Glass Phys. Chem.*, 1997, **23**, 45–57.
79. Fernandes, M. H. V. & Cable, M. Reactive vaporisation of sodium tetraborate with water vapour. *Glass Technol.*, 1993, **34** (1), 26–32.
80. Saringulyan, R. S. Value reported in the SciGlass database, code 3561, GNo. 22935, 1970.
81. Shartsis, L., Capps, W. & Spinner, S. Viscosity and electrical resistivity of molten alkali borates. *J. Am. Ceram. Soc.*, 1953, **36**, 319–26.
82. Gruner, K., Koltermann, M. & Mueller, K. P. Quarzbildung und Kristallisation aus binaeren Lithiumsilicatschmelzen und -gläsern“ (Quartz formation and crystallisation of binary lithium silicate melts and glasses); *Glastech. Ber.*, 1967, **40** (5), 185–94. (In German.)
83. Ahmed, A. A., El-Batal, H. A., Ghoneim, N. A. & Khalifa, F. A. Leaching of some lithium silicate glasses and glass-ceramics by HCl. *J. Non-Cryst. Solids*, 1980, **41** (1), 57–70.
84. Isard, J. O. The mixed alkali effect in glass. *J. Non-Cryst. Solids*, 1969, **1** (3), 235–61.
85. Day, D. E. Mixed alkali glasses - their properties and uses. *J. Non-Cryst. Solids*, 1976, **21** (3), 343–72.
86. LaCourse, W. C. & Cormack, A. N. Structural influences on the mixed alkali effect in glasses. *Trans. Am. Crystallogr. Assoc.*, 1991, **27**, 211–24 (*Proc. Symp. The Structural Chemistry of Silicates*, 22–24 Jul. 1991, Toledo, OH, USA).
87. Leko, V. K. *Inorg. Mater.*, 1967, **3**, 1645.
88. Nemilov, S. U. *Zh. Prikl. Kim. (Leningrad)*, 1969, **42**, 55.
89. Leko, V. K., Gusakova, N. K., Meshcheryakova, E. V. & Prokhorova, T. I. The effect of impurity alkali oxides, hydroxyl groups,  $\text{Al}_2\text{O}_3$ , and  $\text{Ga}_2\text{O}_3$ , on the viscosity of vitreous silica. *Glass Phys. Chem.*, 1977, **3** (3), 204–19; Leko, V. K., Meshcheryakova, E. V., Gusakova, N. K. & Lebedeva, R. B. *Opt. Mekh. Prom.*, 1974, **12**, 42.
90. Avramov, I., Rüssel, C. & Keding, R. Effect of chemical composition on viscosity of oxide glasses. *J. Non-Cryst. Solids*, 2003, **324**, 29–35.
91. Mazurin, O. V. & Gankin, Yu. About testing the reliability of glass property data in binary systems. *J. Non-Cryst. Solids*, 2004, **342**, 166–9.
- Mazurin, O. V. & Gankin, Yu. Determination of the most reliable glass property values by the SciGlass information system. *Proc. CD XX Int. Congr. on Glass*, Kyoto, Japan, 27 Sept.–1 Oct. 2004. Mazurin, O. V. Glass properties: compilation, evaluation, and prediction. *J. Non-Cryst. Solids*, 2005, **351**, 12–13, 1103–12.
92. Data by M. Liska and V. P. Klyuev from the SciGlass Database, private communication, O. V. Mazurin.
93. Data by O. V. Mazurin from the SciGlass Database, private communication.
94. Taylor, N. W. & Dear, P. S. *J. Am. Ceram. Soc.*, 1937, **20** (9), 296.
95. Lee, S.-K., Tatsumisago, M. & Minami, T. *J. Ceram. Soc. Jpn.*, 1993, **101** (9), 1018.
96. Schnaus, U. E., Schroeder, J. & Haus, J. W. *Phys. Lett. A*, 1976, **57** (1), 92.
97. El-Badry, Kh. & Ghoneim, N. A. *Glastech. Ber.*, 1983, **56K** (2), 975; El-Badry, Kh. & Ghoneim, N. A. *Cent. Glass Ceram. Res. Inst. Bull.*, 1982, **29** (3), 72.
98. Jenckel, E. & Schwittman, A. *Glastech. Ber.*, 1938, **16** (5), 163.
99. Stolyar, S. V. & Besedina, S. A. *Fiz. Khim. Stekla*, 1992, **18** (3), 88.
100. Ehrst, D., Leister, M., Matthai, A., Ruessel, C. & Breitbarth, F. *Proc. Fourth Int. Conf. Fundamentals of Glass Science and Technology*, Sweden, 1997, 204.
101. Ammar, M. M., El-Badry, Kh. & Gharib, S. *Egypt. J. Phys.*, 1977, **8** (1), 1.
102. Data by Kanchieva from the SciGlass Database. private communication, O. V. Mazurin.
103. Evstropiev, K. S. *Izv. Akad. Nauk SSSR*, 1940, **4** (4), 616.
104. Plumat, E. *Silicates Ind.*, 1956, **21** (10), 391.
105. Ivanov, O. G., Tretjakova, N. I. & Mazurin, O. V. *Steklo Keram.*, 1969, **7**, 42; Tretjakova, N. I. & Mazurin, O. V. *Vliyanie Okislov Dvukhvalentnykh Metallov na Vyzkost Prostykh Silikatnykh Stekol*. Deposited in VINITI, Moscow, No. 995-69 Dep., 1969.
106. Data by P. Jarry from the SciGlass Database, private communication, O. V. Mazurin.
107. Taylor, T. D. & Rindone, G. E. *J. Am. Ceram. Soc.*, 1970, **53** (12), 692.
108. Hoffmann, L. C., Kupinski, T. A., Thakur, R. L. & Weyl, W. A. *J. Soc. Glass Technol.*, 1952, **36**, 196–216.
109. Hanson, C. D. & Egami, T. Distribution of  $\text{Cs}^+$  ions in single and mixed alkali silicate glasses from energy dispersive x-ray diffraction. *J. Non-Cryst. Solids*, 1986, **87** (1–2), 171–84.
110. Berg, G. & Ludwig, A. Mixed oxide effect in an ion-exchanged glass. *J. Non-Cryst. Solids*, 1994, **170** (1), 109–11.
111. Tomandl, G. & Schaeffer, H. A. The mixed-alkali effect - a permanent challenge. *J. Non-Cryst. Solids*, 1985, **73**, 179–96. Tomandl, G. & Schaeffer, H. A. *Non-Crystalline Solids*. Edited by G. H. Frischat, Trans Tech Publications, Bay Village, Ohio, 1977, 480.
112. Kim, K.-D. & Hwang, J.-H. Influence of  $\text{BaO}/(\text{SrO}+\text{BaO})$  on some thermal properties of  $\text{R}_2\text{O}-\text{RO}-\text{SiO}_2$  glasses for plasma display panel substrate. *Glastech. Ber., Glass Sci. Technol.*, 1999, **72** (12), 393–7.
113. Waesche, R. & Brueckner, R.  $T_g$  ultraviolet-transparency and mixed oxide effect of ultrapure ternary alkaline earth-metaphosphate glasses. *J. Non-Cryst. Solids*, 1989, **107** (2–3), 309–15.
114. Shelby, J. E. & Ortolano, R. L. Properties and structure of  $\text{NaF}-\text{Na}_2\text{O}-\text{B}_2\text{O}_3$  glasses. *Phys. Chem. Glasses*, 1990, **31** (1), 25–9.
115. Shelby, J. E. & McVay, G. L. Influence of water on the viscosity and thermal expansion of sodium trisilicate glasses. *J. Non-Cryst. Solids*, 1976, **20** (3), 439–49.
116. Prasad, P. S. S., Rani, A. N. D. & Radhakrishna, S. Mixed glass former effect in  $\text{AgI}-\text{Ag}_2\text{O}-\text{V}_2\text{O}_5-\text{P}_2\text{O}_5$  quaternary amorphous solid electrolytes. *Mater. Chem. Phys.*, 1990, **25** (5), 487–99.
117. Lapp, J. C. & Shelby, J. E. The mixed alkali effect in sodium and potassium galliosilicate glasses. Part 1. Glass transformation temperatures. *J. Non-Cryst. Solids*, 1986, **84** (1–3), 463–7. Lapp, J. C. & Shelby, J. E. The mixed alkali effect in sodium and potassium galliosilicate glasses. Part 2. DC electrical conductivity. *J. Non-Cryst. Solids*, 1986, **86** (3), 350–60.
118. Ghosh, S. & Ghosh, A. Ion dynamics and mixed mobile ion effect in fluoride glasses. *J. Appl. Phys.*, 2005, **97** (12), 123525.
119. Brook, H. C., Chadwick, A. V., Mosslemans, J. F. W. & Greaves, G. N. EXAFS study of a ‘mixed-alkali’ type effect in sodium-calcium borate glass. *Rad. Effects Defects Solids*, 1999, **150** (1–4 pt. 2), 795/403–799/407.
120. Kim, K.-D. & Lee, S.-H. Viscosity behaviour and mixed alkali effect of alkali aluminosilicate glass melts. *J. Ceram. Soc. Jpn.*, 1997, **105** (1226), 827–32.
121. Ivanov, A. O. *Sov. Phys.-Solid State*, 1964, **5**, 1933. Data also reported by Isard.
122. Shelby, J. E. *Handbook of Gas Diffusion in Solids and Melts*. ASM International, ISBN: 0871705664, 1996.
123. Gonzalez-Oliver, C. J. R., Johnson, P. S. & James, P. F. Influence of water content on the rates of crystal nucleation and growth in lithia-silica and soda-lime-silica glasses. *J. Mater. Sci.*, 1979, **14** (5), 1159.